

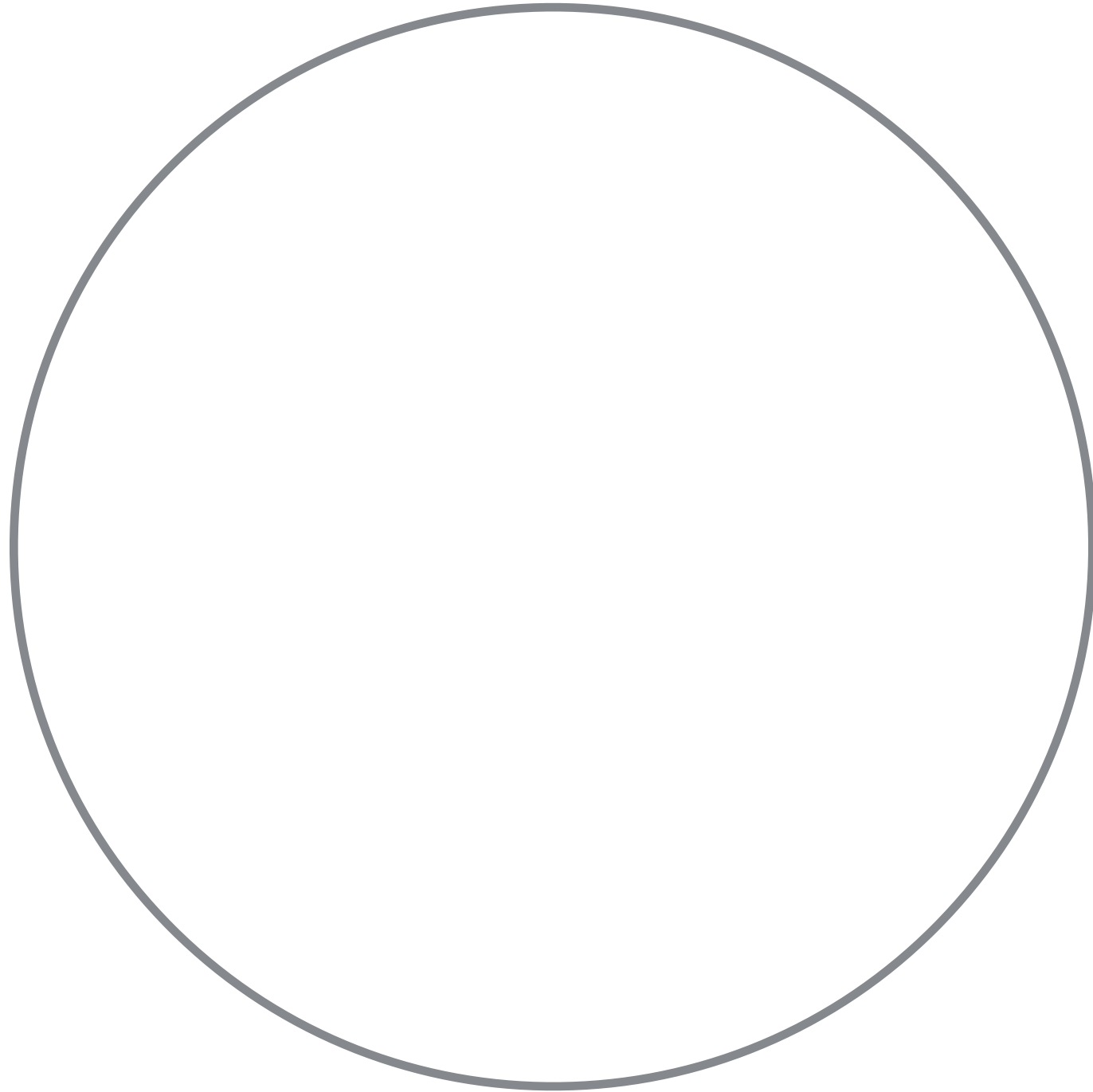
Experimental Limits on Gravitational Waves in the MHz Frequency Range with the Fermilab Holometer

Robert Lanza
The University of Chicago
2015-03-27

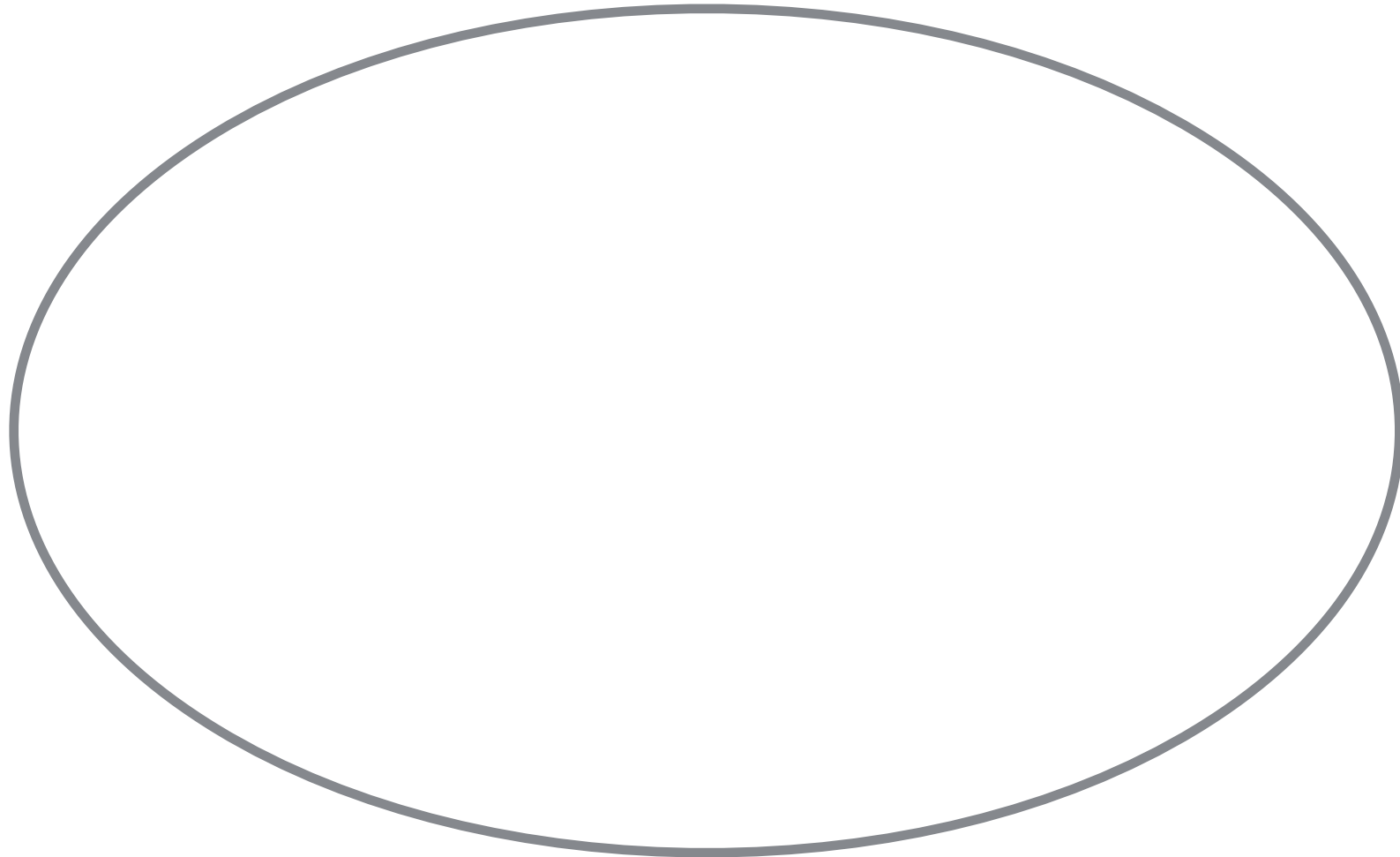
Overview

- Context For This Work (Gravitational Waves and Detectors)
- The Holometer Instrument
- Dominant Noise Sources
- End-To-End Calibration
- Analysis and Results

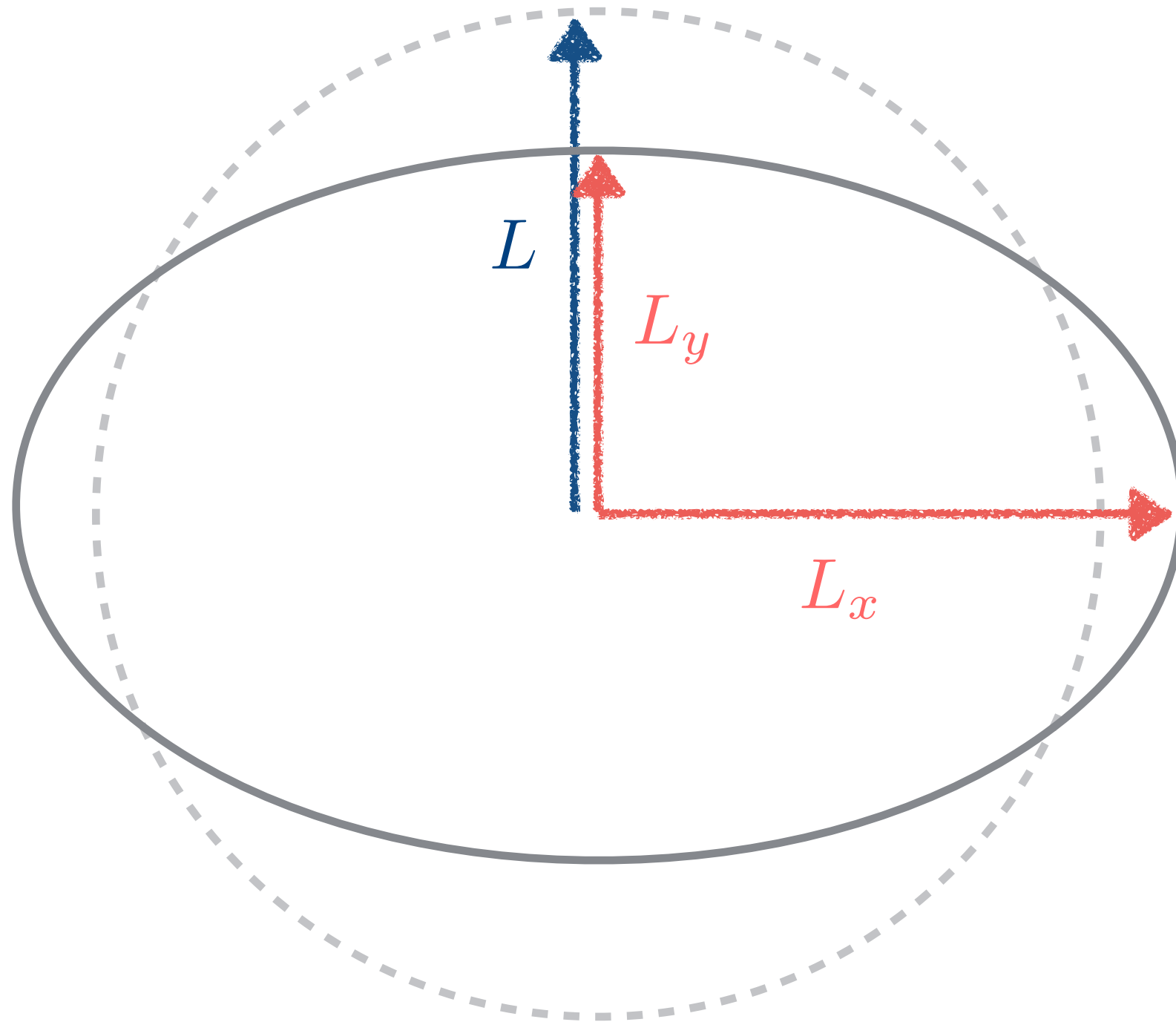
Gravitational Waves



Gravitational Waves

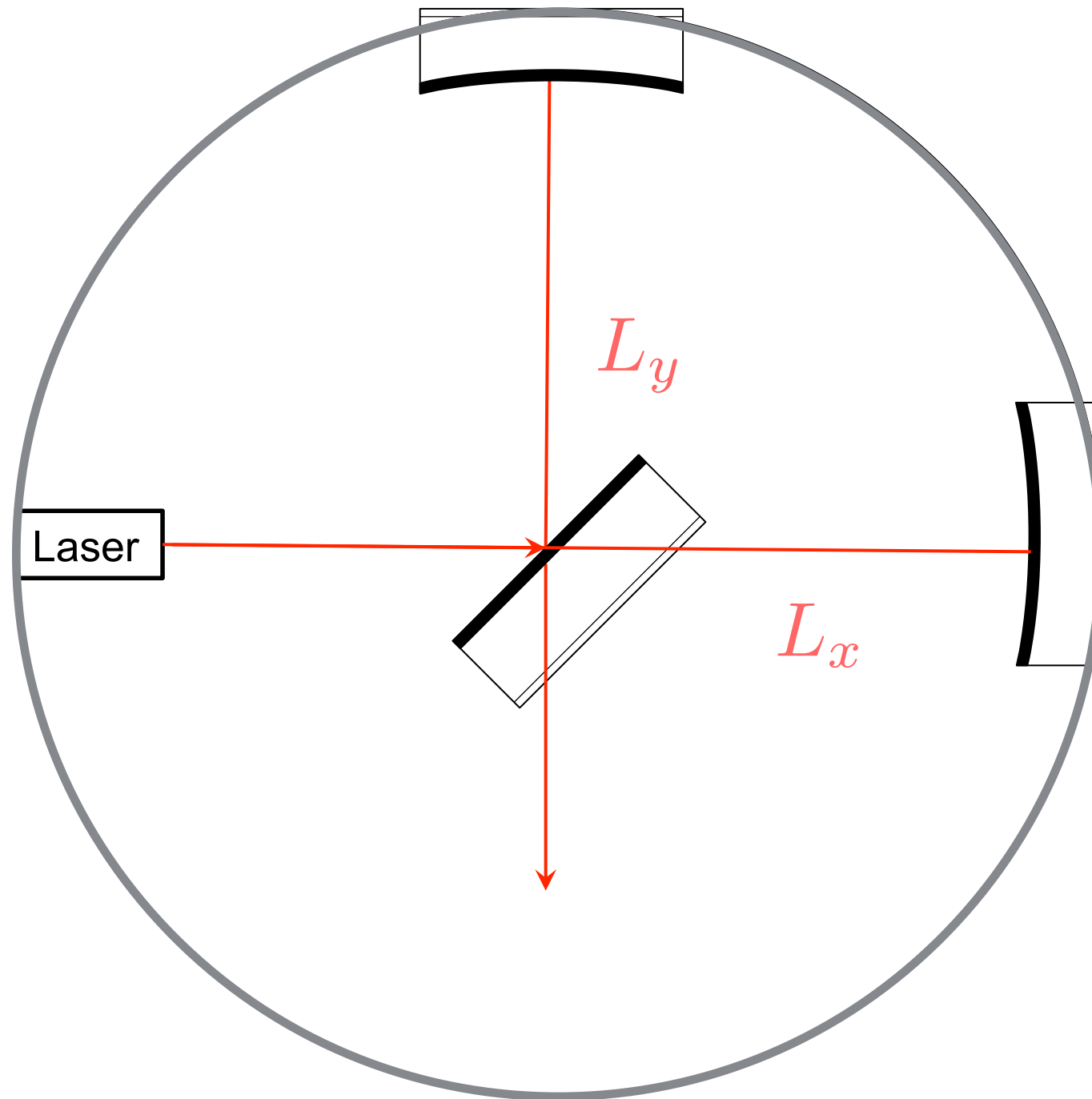


New limits are placed on the GW strain $h(f = 1\text{MHz} - 11\text{MHz})$



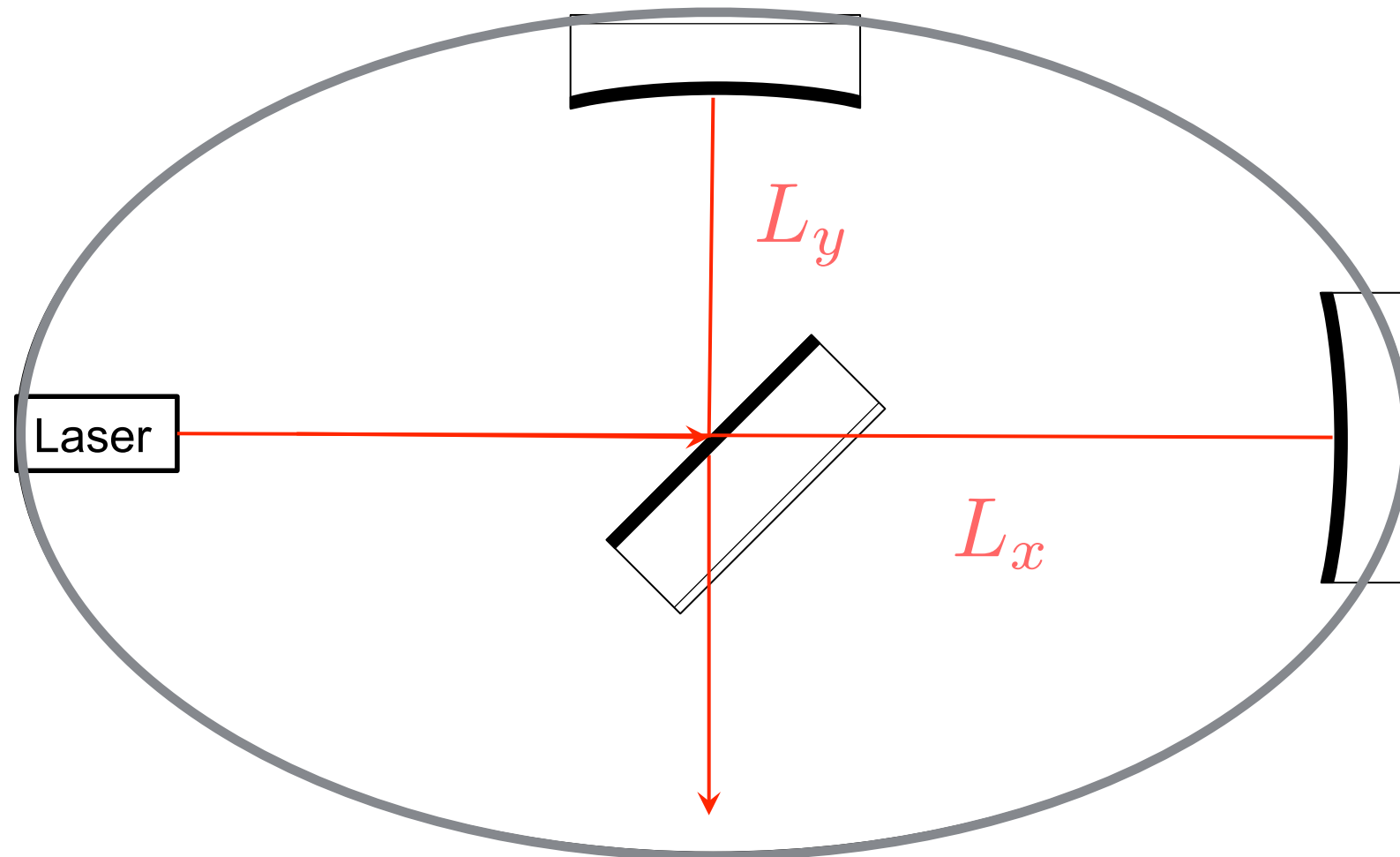
$$L_x - L_y = hL$$

Detecting Gravitational Waves



$$L_x - L_y = hL$$

Detecting Gravitational Waves



$$L_x - L_y = hL$$

Some Context: Where The New Results Fit In

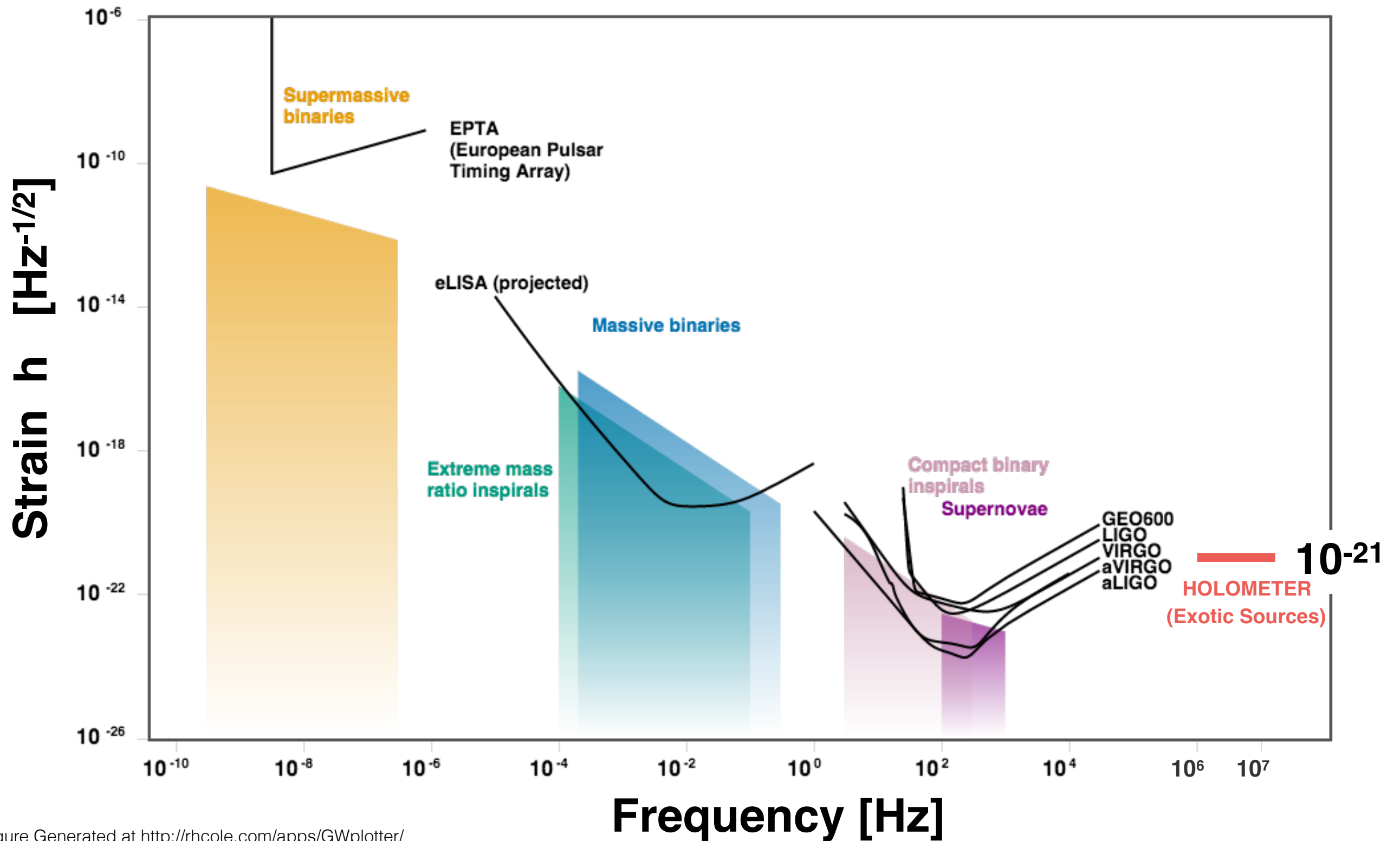


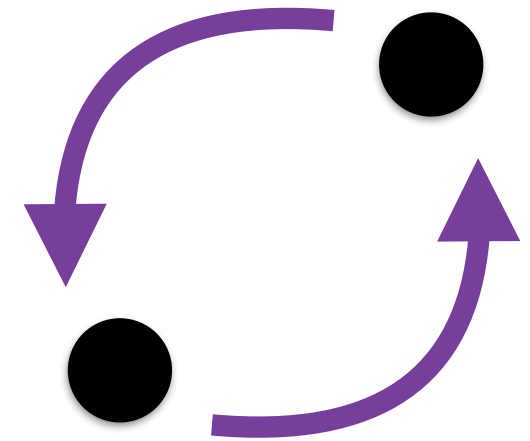
Figure Generated at <http://rhcole.com/apps/GWplotter/>
 See also: C J Moore et al 2015 Class. Quantum Grav. 32 015014
 doi:10.1088/0264-9381/32/1/015014

Exotic Sources of Megahertz Gravitational Waves

Tiny black hole binaries

Small black holes can have very short period orbits. As an example, a pair of ~ 3 micron size black holes orbiting ~ 10 cm apart radiate \sim MHz waves; they produce a detectable periodic (monochromatic) signal in our apparatus if they lie within the solar system.

MHz black holes must be much smaller and denser than stellar mass black holes ($<$ meters instead of $>$ km); they can only be created in exotic high density conditions of early universe.

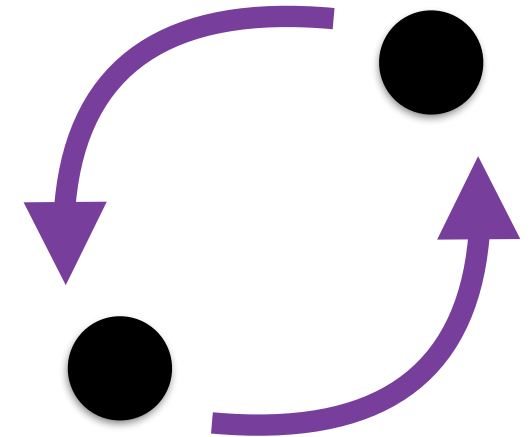


Exotic Sources of Megahertz Gravitational Waves

Tiny black hole binaries

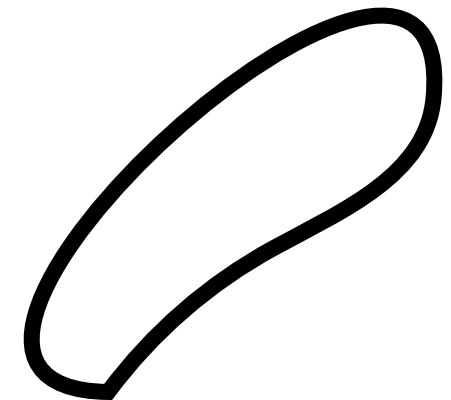
Small black holes can have very short period orbits. As an example, a pair of ~ 3 micron size black holes orbiting ~ 10 cm apart radiate \sim MHz waves; they produce a detectable periodic (monochromatic) signal in our apparatus if they lie within the solar system.

MHz black holes must be much smaller and denser than stellar mass black holes ($<$ meters instead of $>$ km); they can only be created in exotic high density conditions of early universe.



Loops of cosmic superstring

In string theory and some field theories, the early universe naturally leaves behind large loops of an exotic new form of energy, “superstrings” that oscillate near the speed of light. A loop of ~ 40 meter size would radiate a harmonic spectrum with a fundamental period in our band. The strength of its gravitational radiation depends on a poorly constrained fundamental parameter, the tension or mass per length of the string. To be detectable here, it typically also has to be within the solar system.

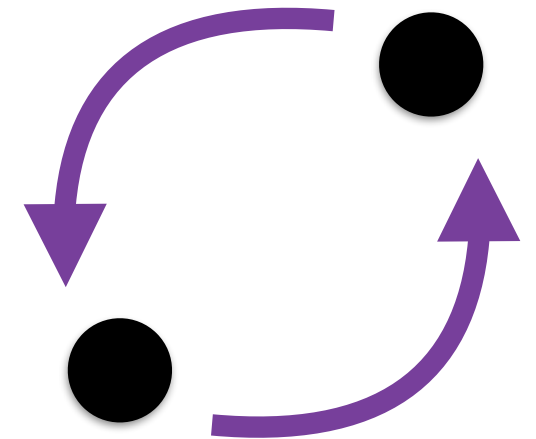


Exotic Sources of Megahertz Gravitational Waves

Tiny black hole binaries

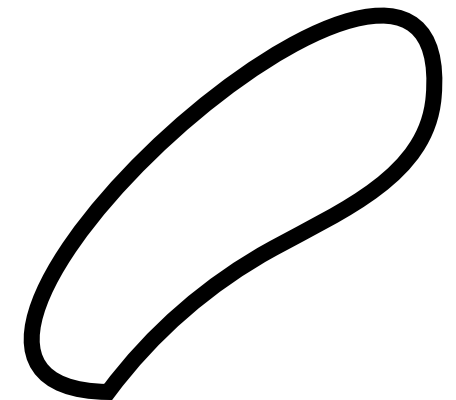
Small black holes can have very short period orbits. As an example, a pair of ~ 3 micron size black holes orbiting ~ 10 cm apart radiate \sim MHz waves; they produce a detectable periodic (monochromatic) signal in our apparatus if they lie within the solar system.

MHz black holes must be much smaller and denser than stellar mass black holes ($<$ meters instead of $>$ km); they can only be created in exotic high density conditions of early universe.



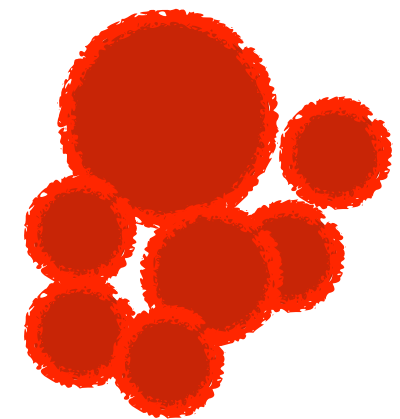
Loops of cosmic superstring

In string theory and some field theories, the early universe naturally leaves behind large loops of an exotic new form of energy, “superstrings” that oscillate near the speed of light. A loop of ~ 40 meter size would radiate a harmonic spectrum with a fundamental period in our band. The strength of its gravitational radiation depends on a poorly constrained fundamental parameter, the tension or mass per length of the string. To be detectable here, it typically also has to be within the solar system.



Flows of energy in the very early Universe

Under some conditions, an expanding universe can undergo a catastrophic phase transition. Roiling flows of relativistic matter can radiate and fill the whole universe with powerful gravitational waves. If this happens around the GUT era, they get redshifted into our observing band. To be detectable in our apparatus, the total energy in this background would then already have been detected by its overall gravity, unless it were concentrated in a narrow band.



The Holometer Instrument

The Holometer Instrument

Fermilab



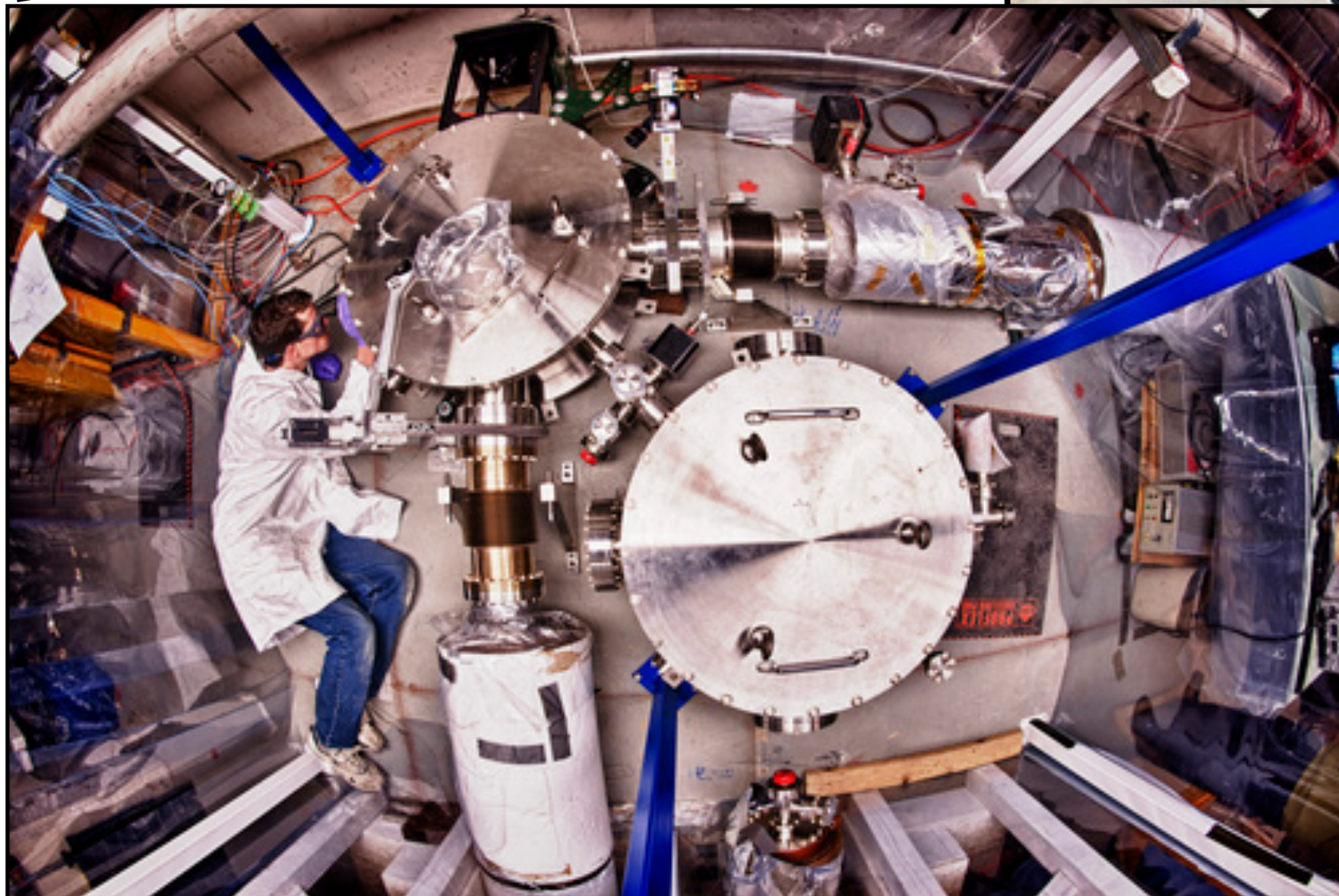
MP8 Meson Beamline



The Holometer Instrument



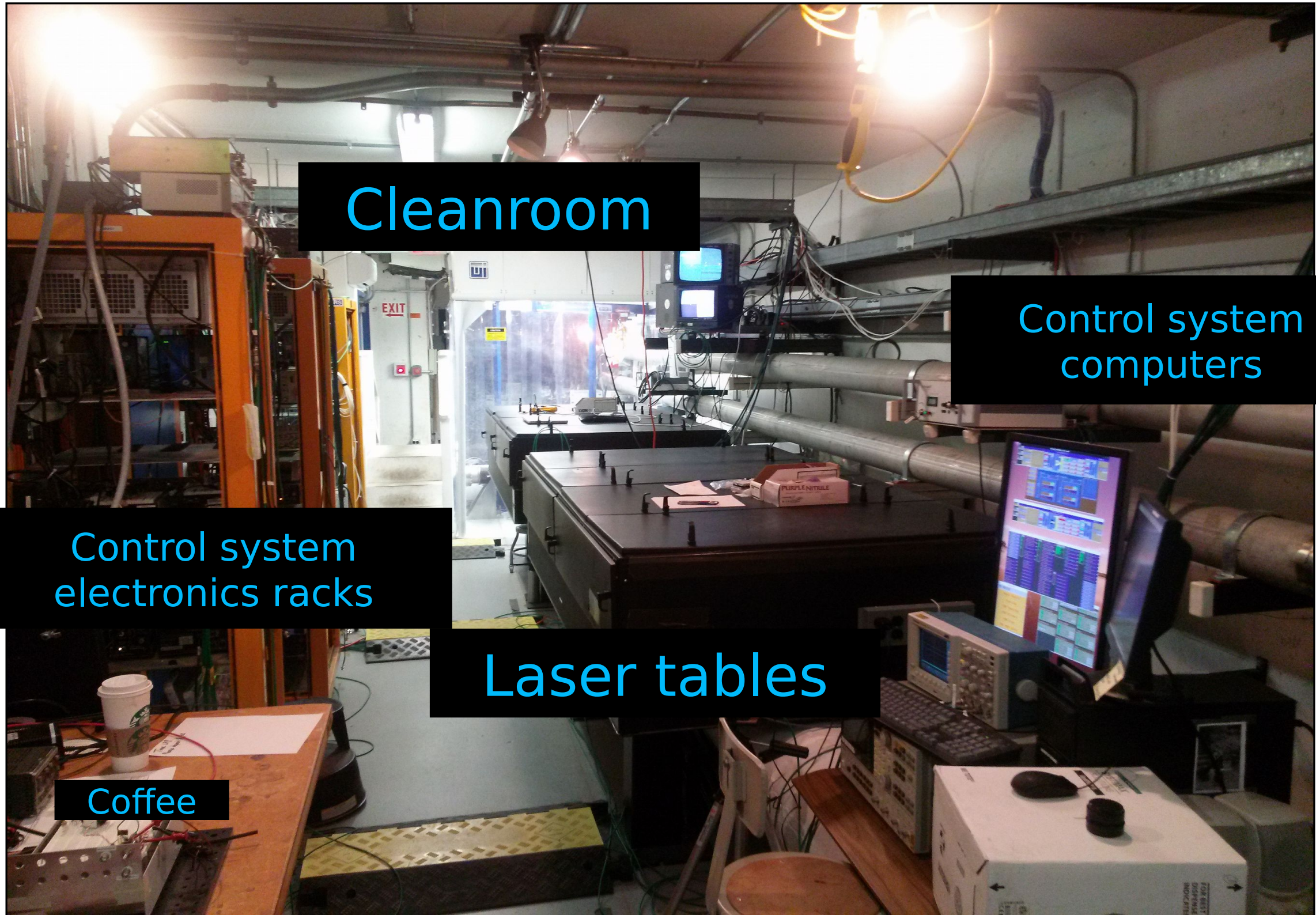
Fermilab



Vertex - Looking Down

The Holometer Instrument

Inside the MP8 Tunnel



Cleanroom

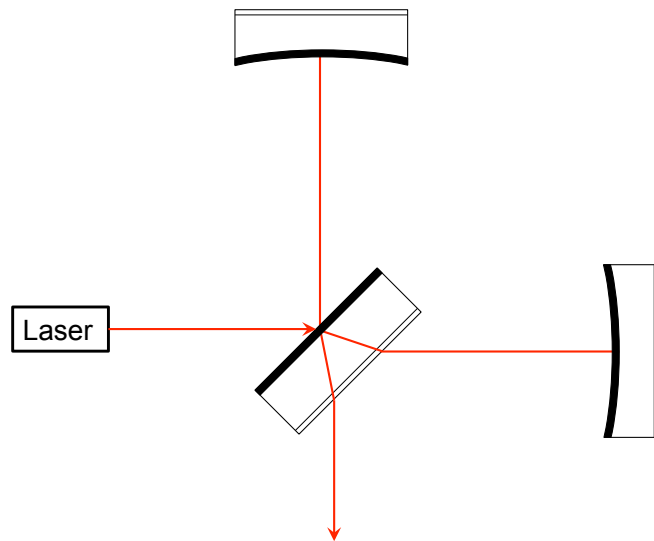
Control system computers

Control system electronics racks

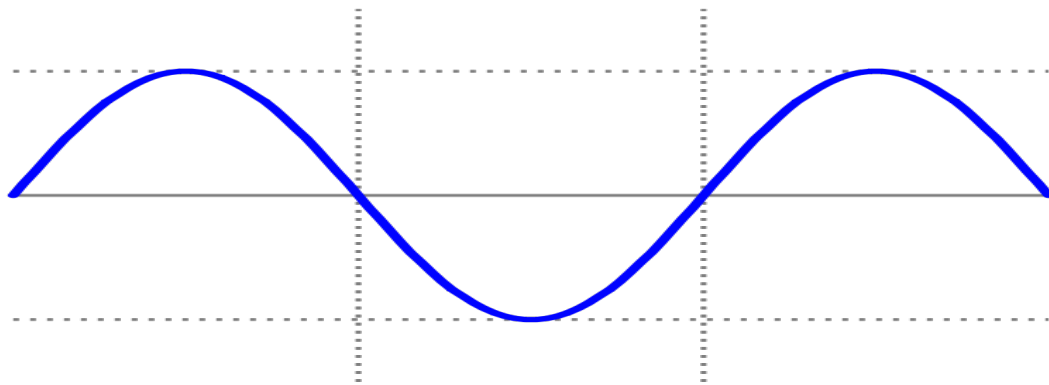
Laser tables

Coffee

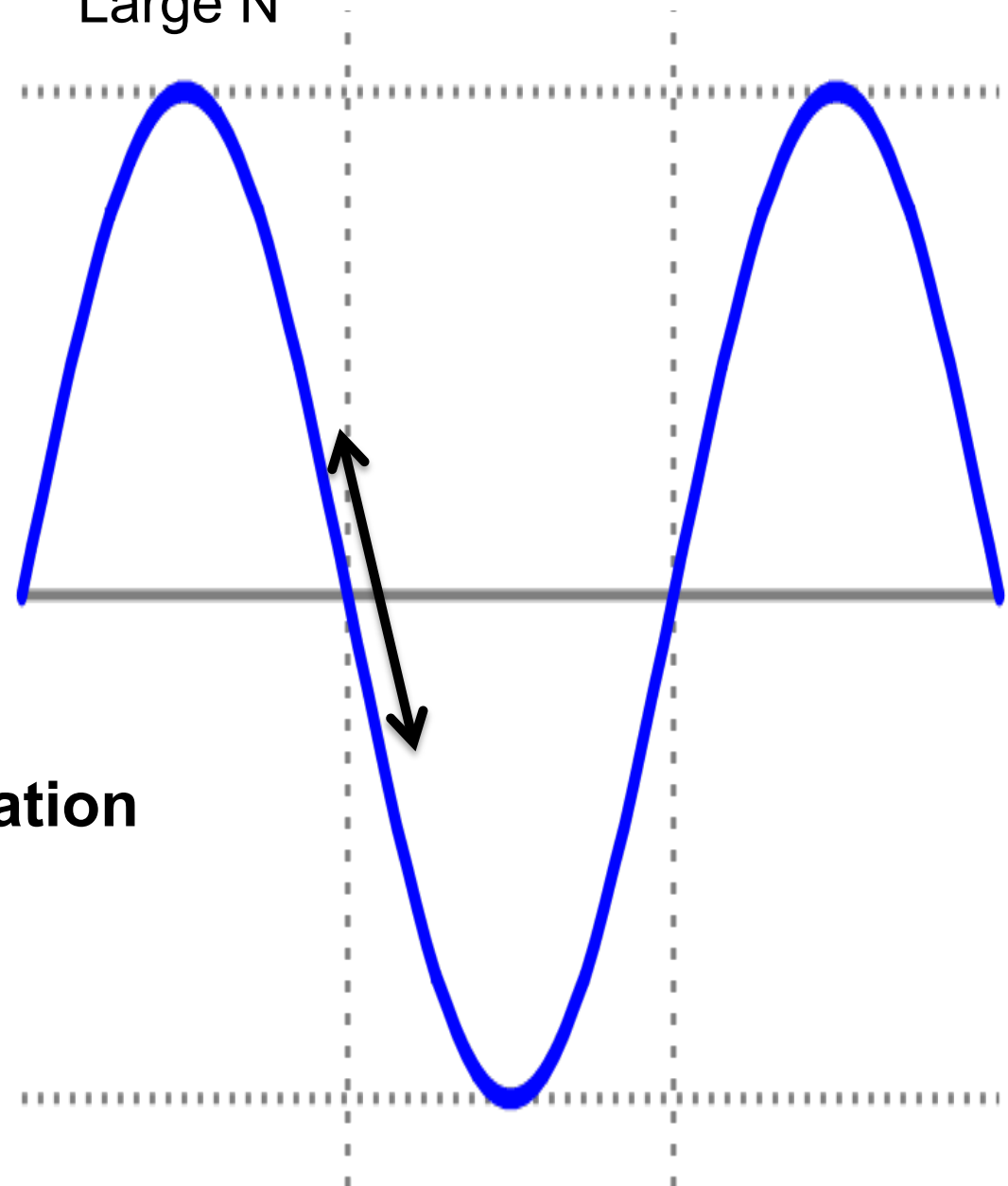
Position Resolution Depends ONLY on Photon Flux. More Photons → Sharper Fringes



Small N



Large N



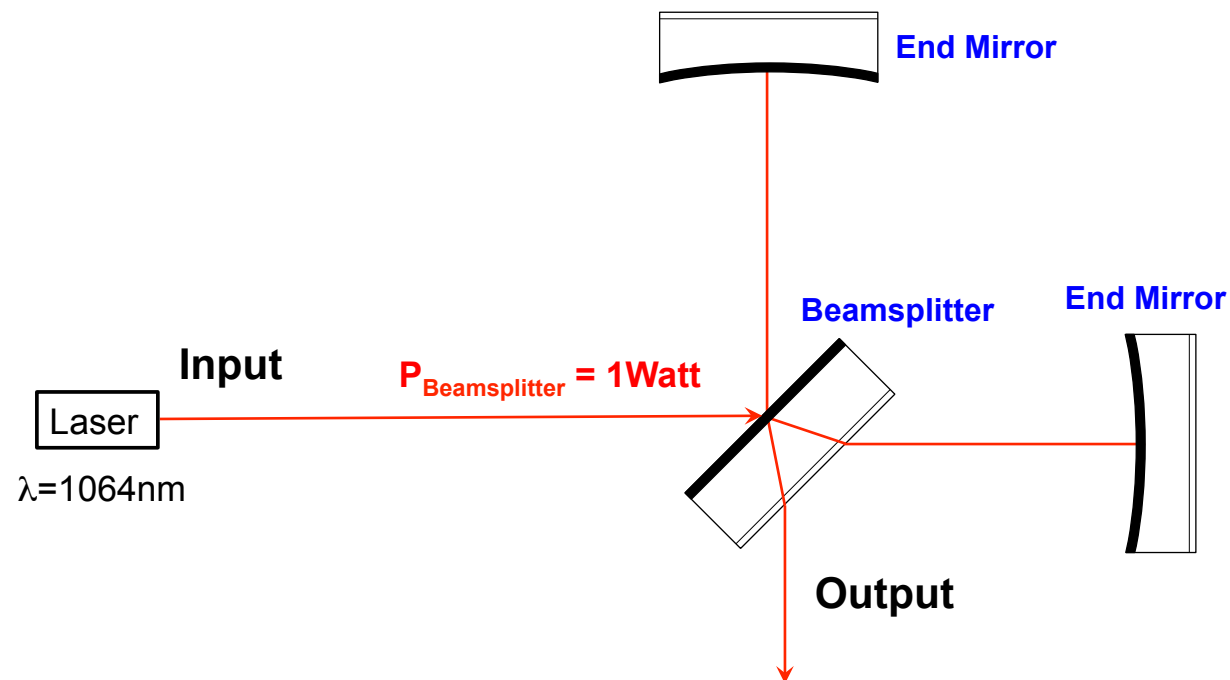
Photon number-phase uncertainty relation
 $\Delta N \times \Delta \phi = 1/2$

$$\Delta x = \Delta \phi \times \frac{\lambda}{2\pi} = \left(\frac{1}{2\sqrt{N}} \right) \times \frac{\lambda}{2\pi}$$

Shot Noise Limited Sensitivity

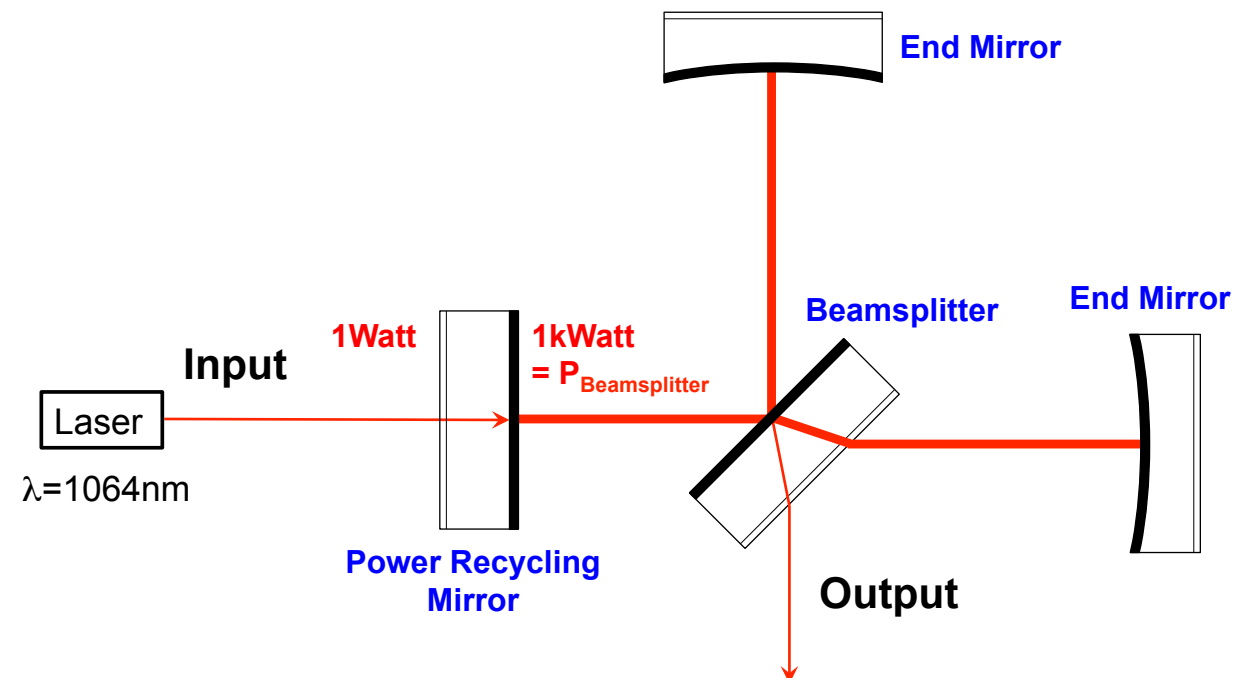
Michelson

Power-Recycled Michelson



Shot noise limited differential arm length sensitivity:

$$\Delta x_{\text{shot}} = \frac{1}{2\pi} \sqrt{\frac{hc\lambda}{P_{\text{Beamsplitter}}}}$$
$$= 7 \times 10^{-17} \text{ m} / \sqrt{\text{Hz}}$$



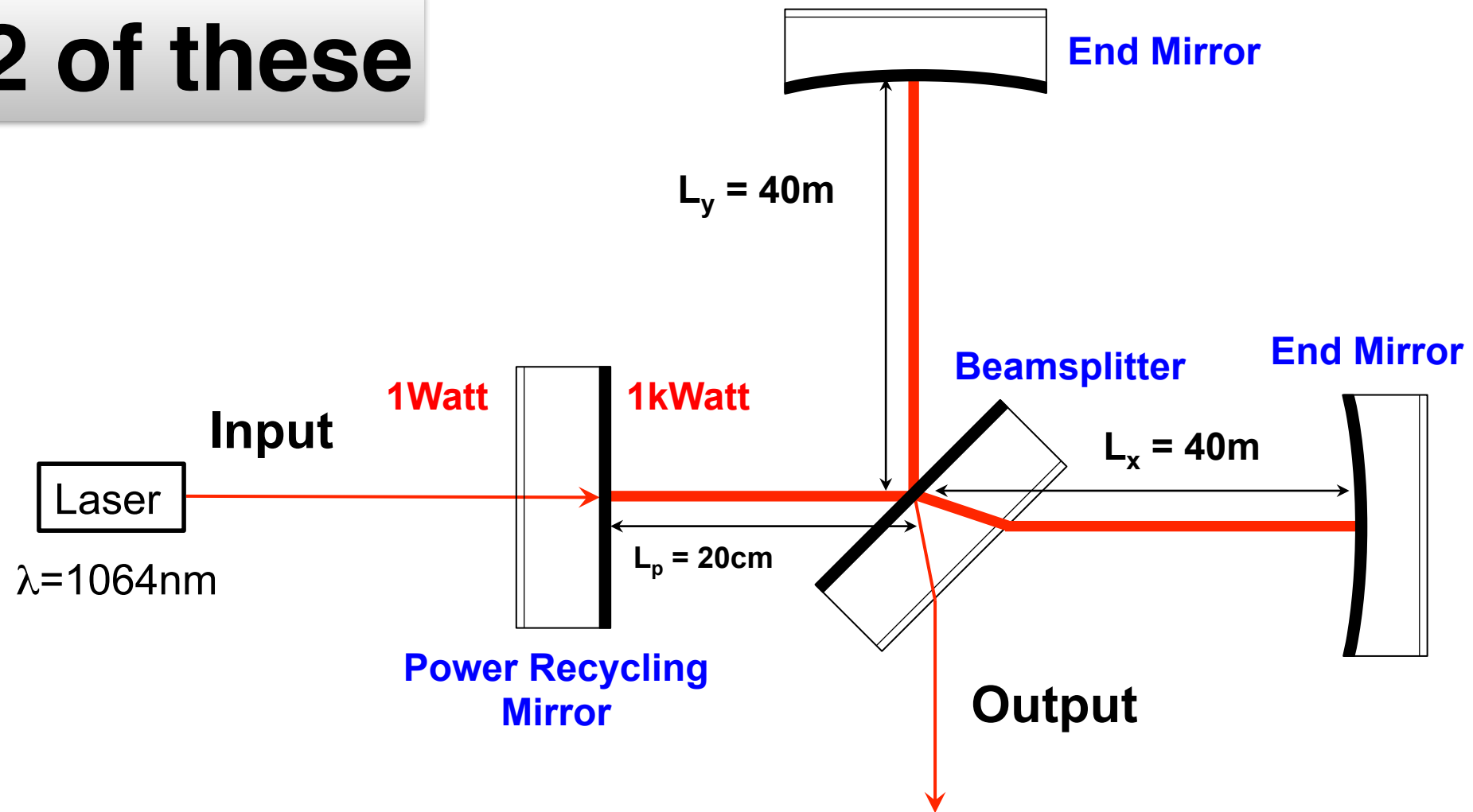
Shot noise limited differential arm length sensitivity:

$$\Delta x_{\text{shot}} = \frac{1}{2\pi} \sqrt{\frac{hc\lambda}{P_{\text{Beamsplitter}}}}$$
$$= 2 \times 10^{-18} \text{ m} / \sqrt{\text{Hz}}$$

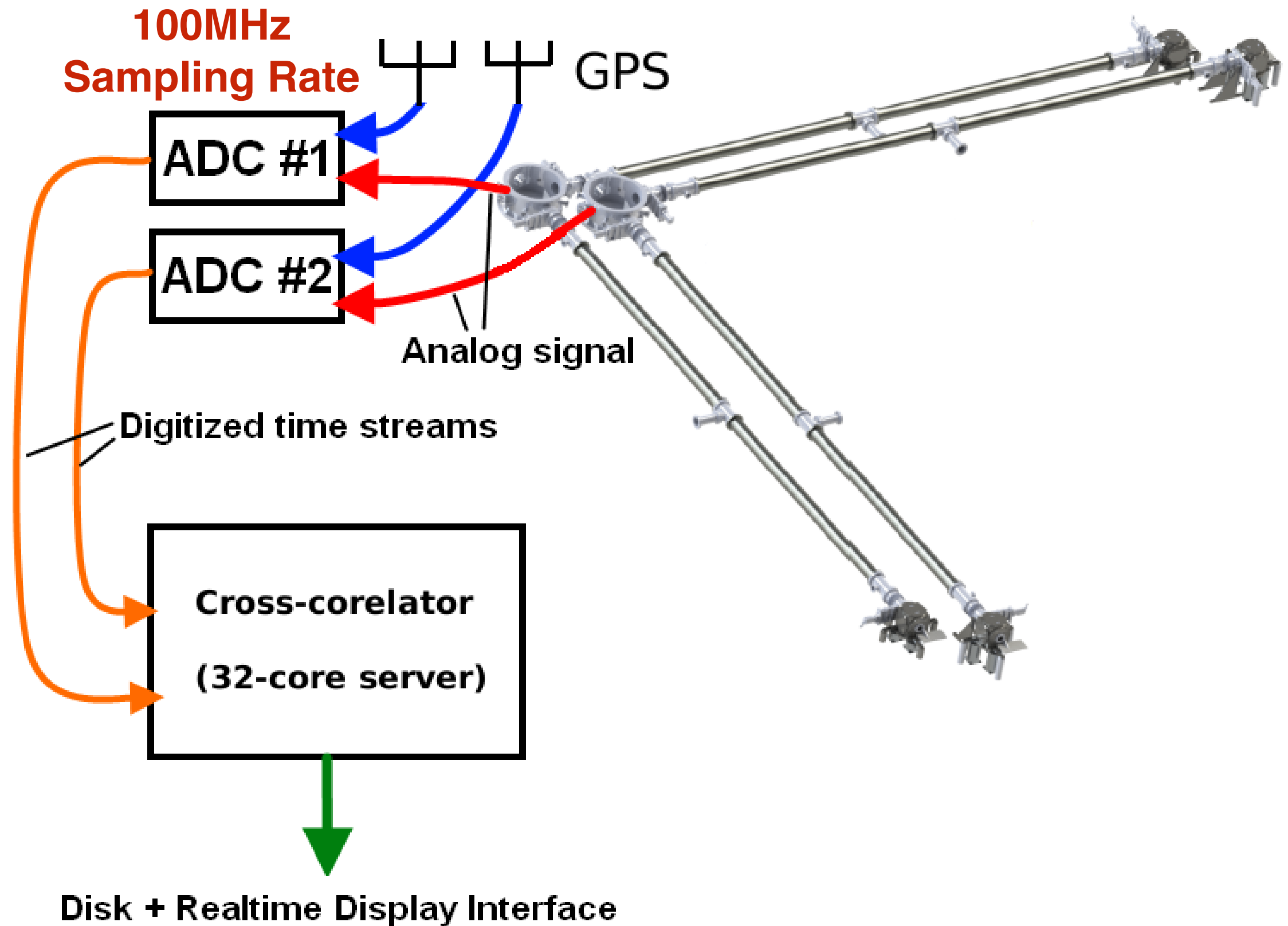
Typical Holometer Operation

The Holometer Instrument

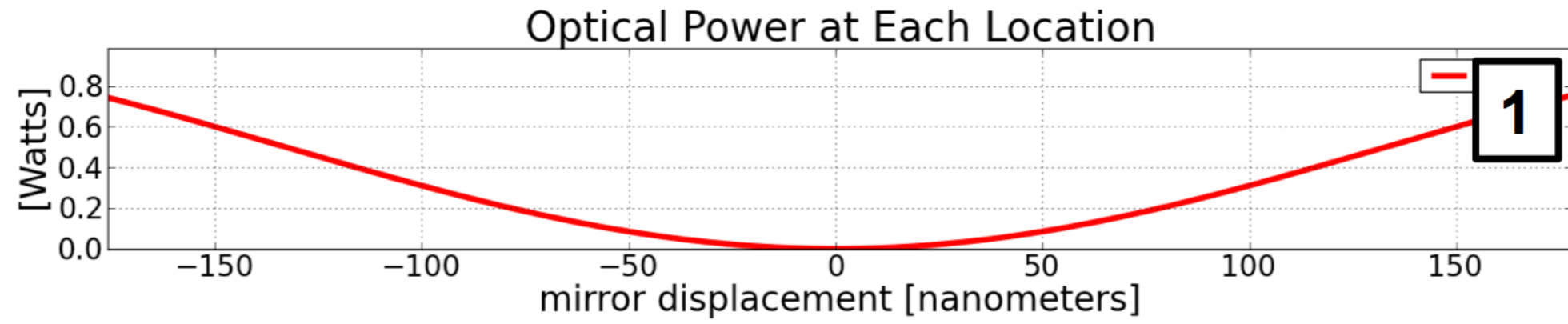
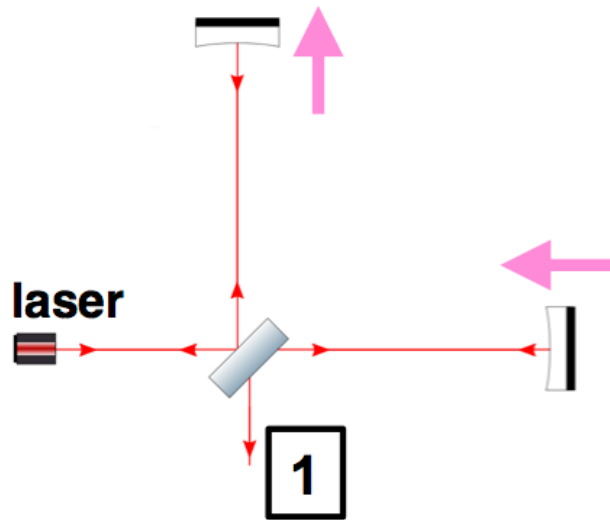
2 of these



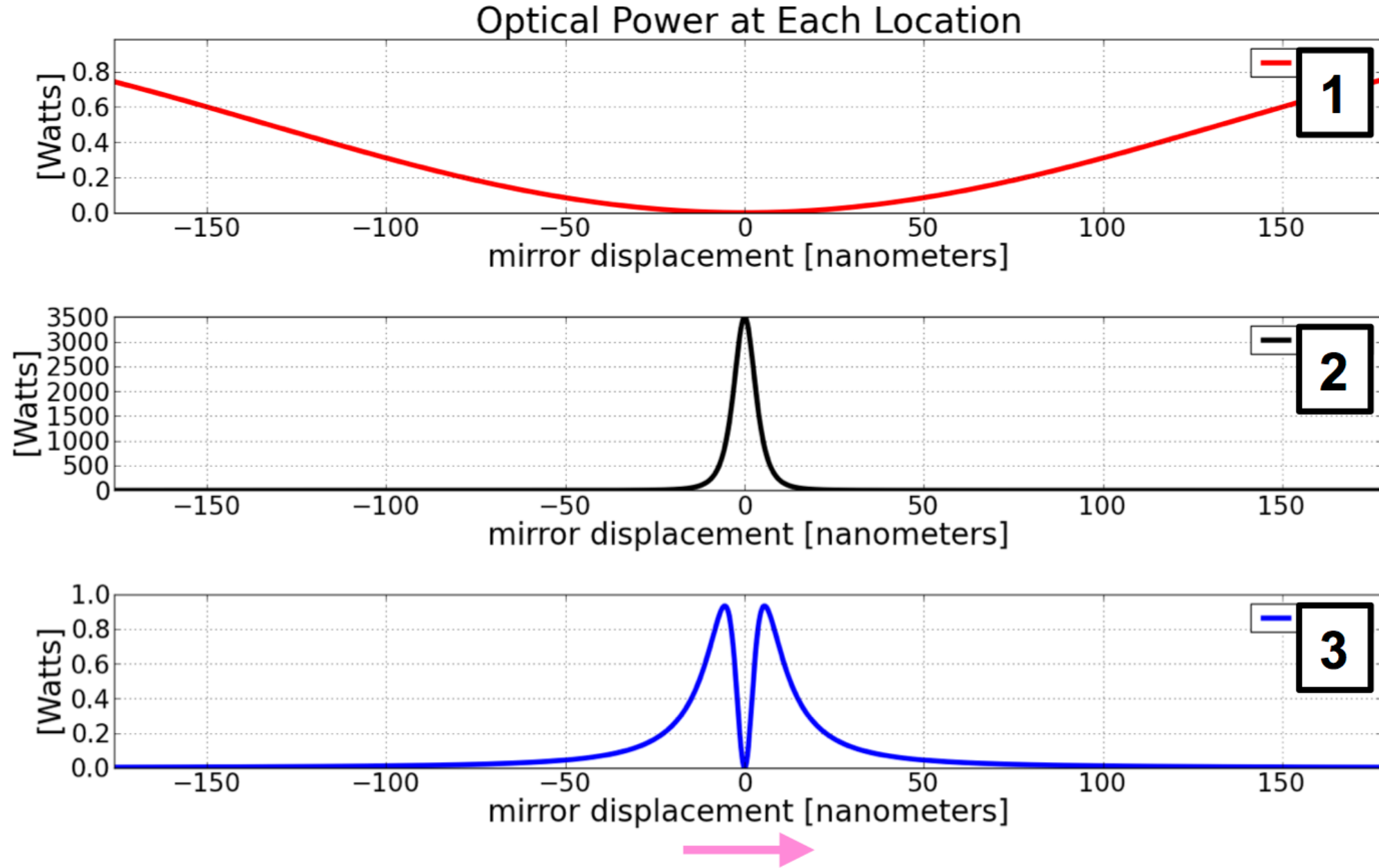
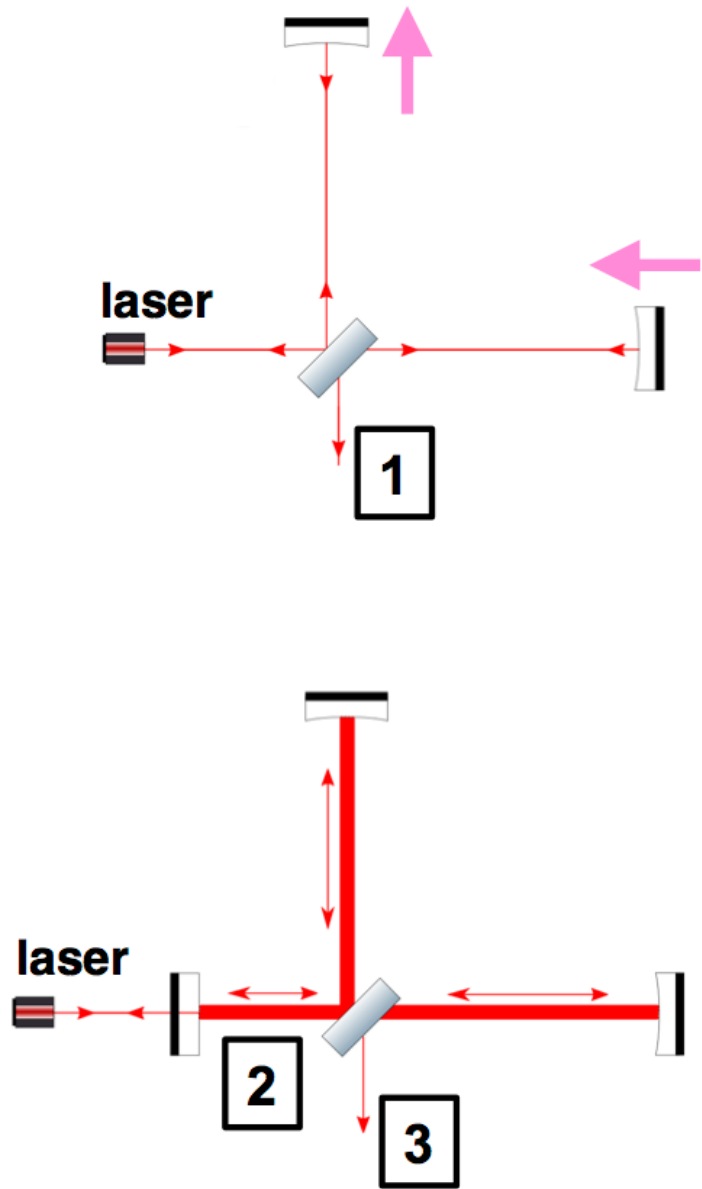
High Frequency Data Acquisition System



Interferometer Signals vs. Differential Arm Length

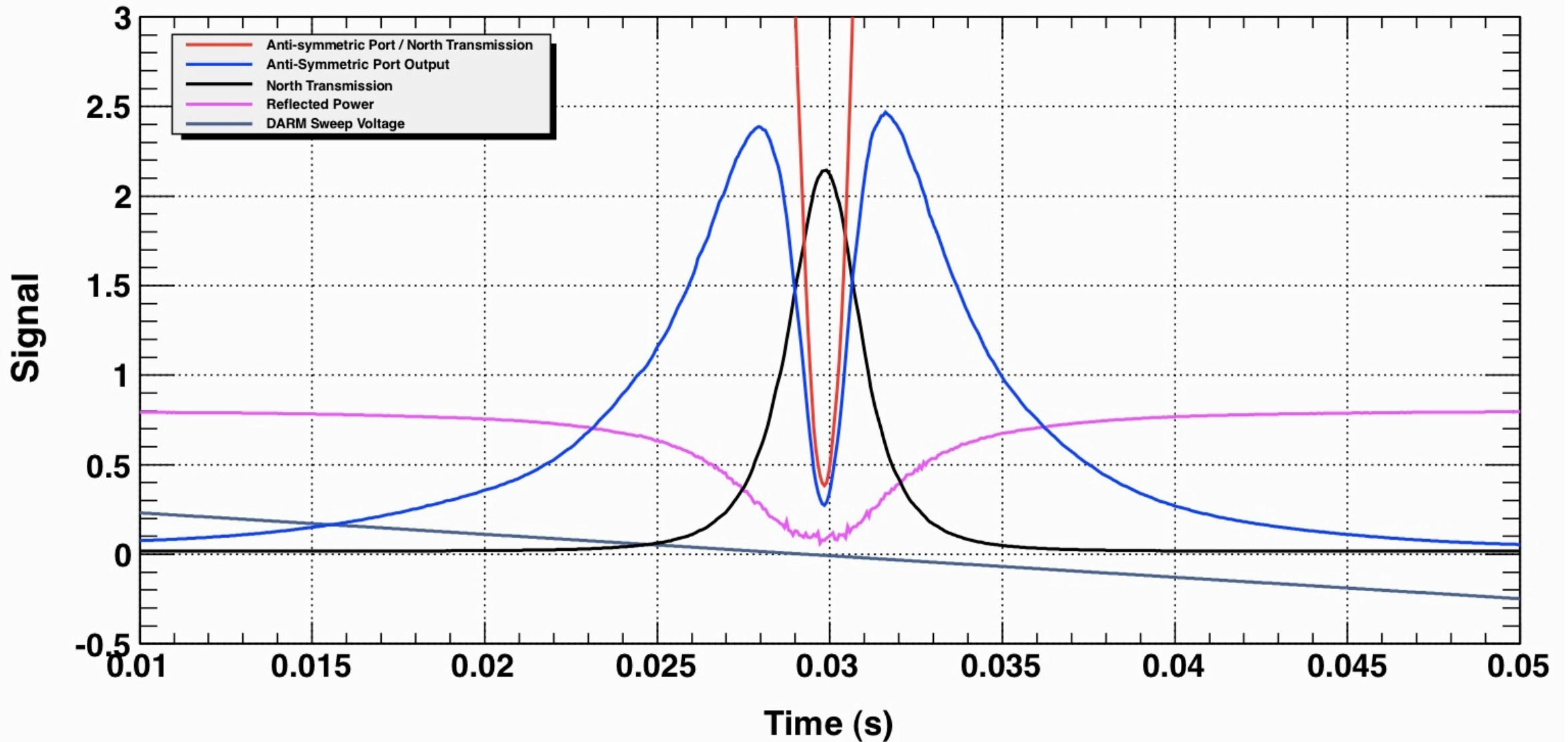


Interferometer Signals vs. Differential Arm Length



Measured Interferometer Signals vs. Differential Arm Length

Time series: Differential Arm Length Sweep



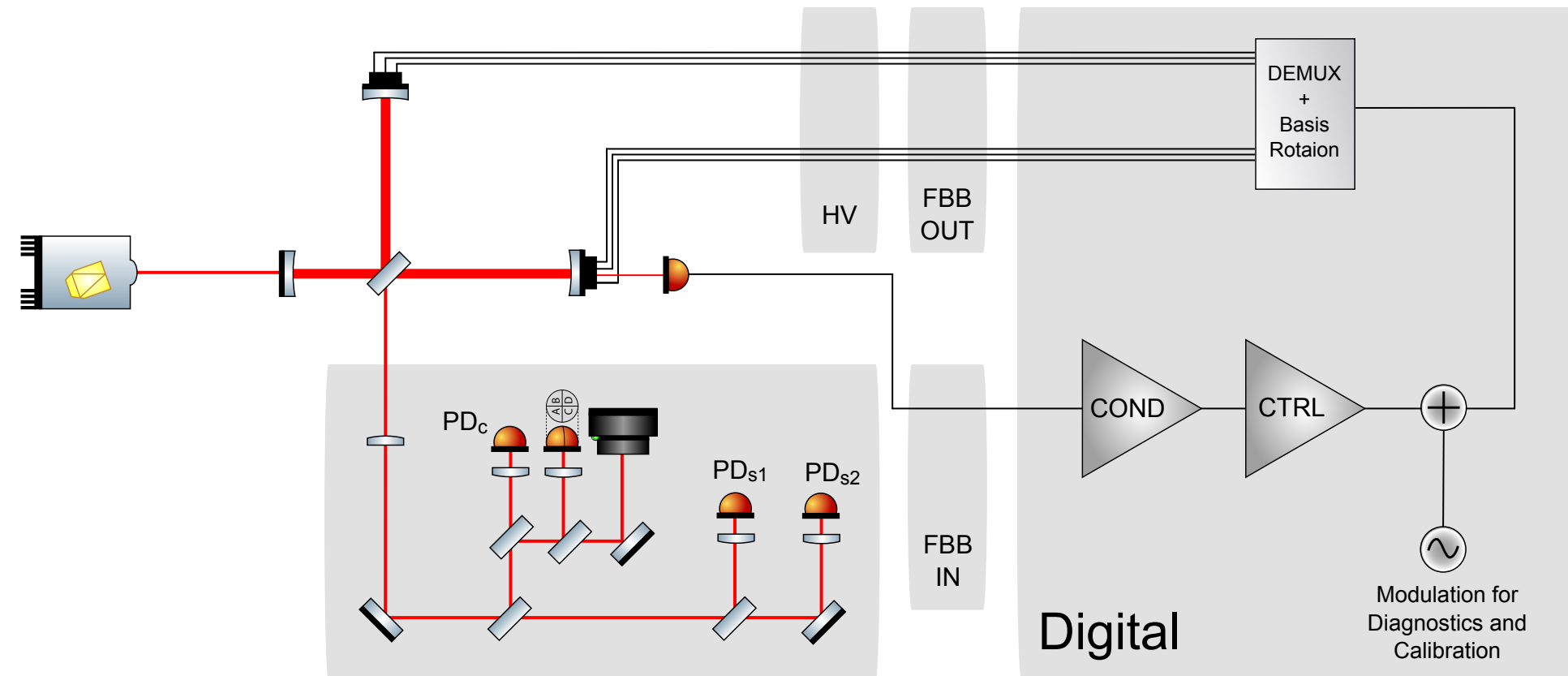
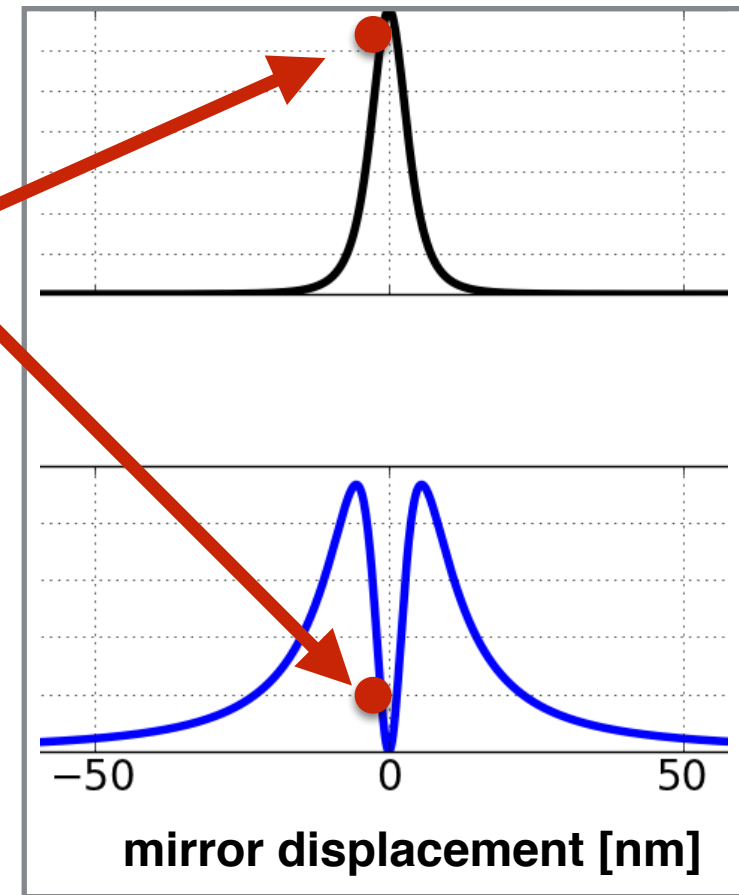
T0=06/04/2013 05:22:11

Avg=1

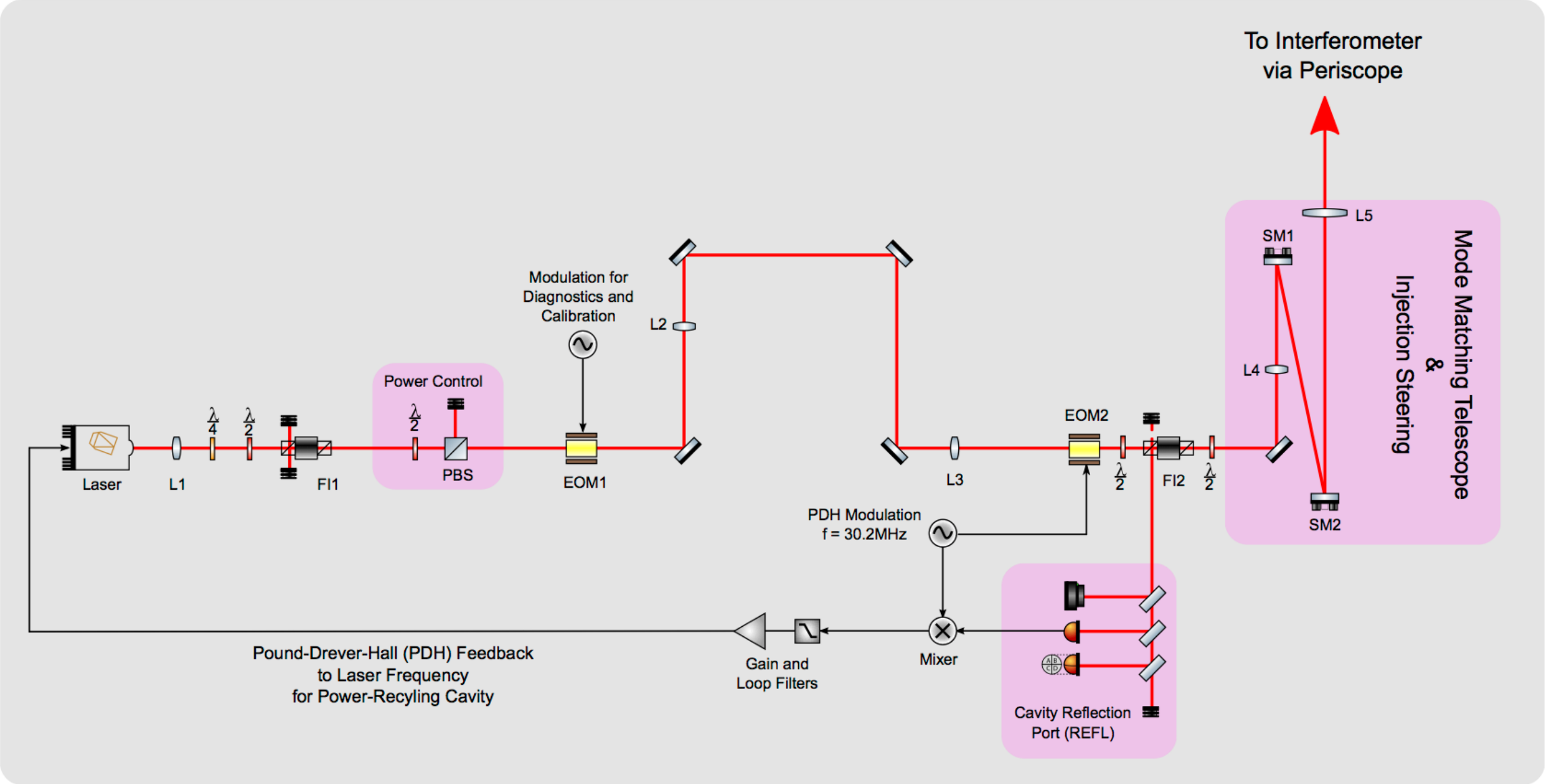
Differential Arm (DARM) Feedback and Control

DARM is edge-locked to transmitted cavity power for easier acquisition

Lock Point



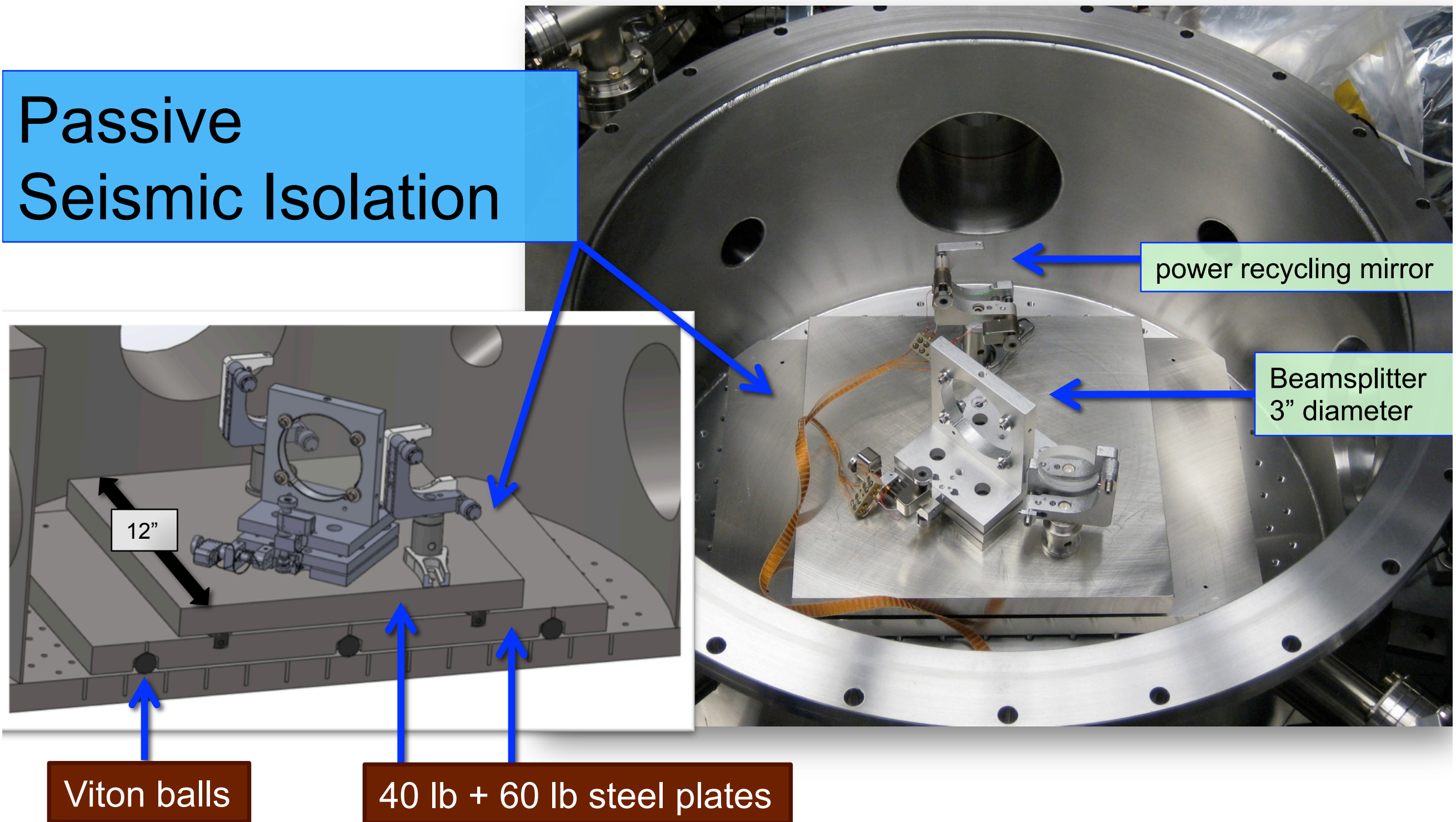
Laser Launch



Dominant Noise Sources

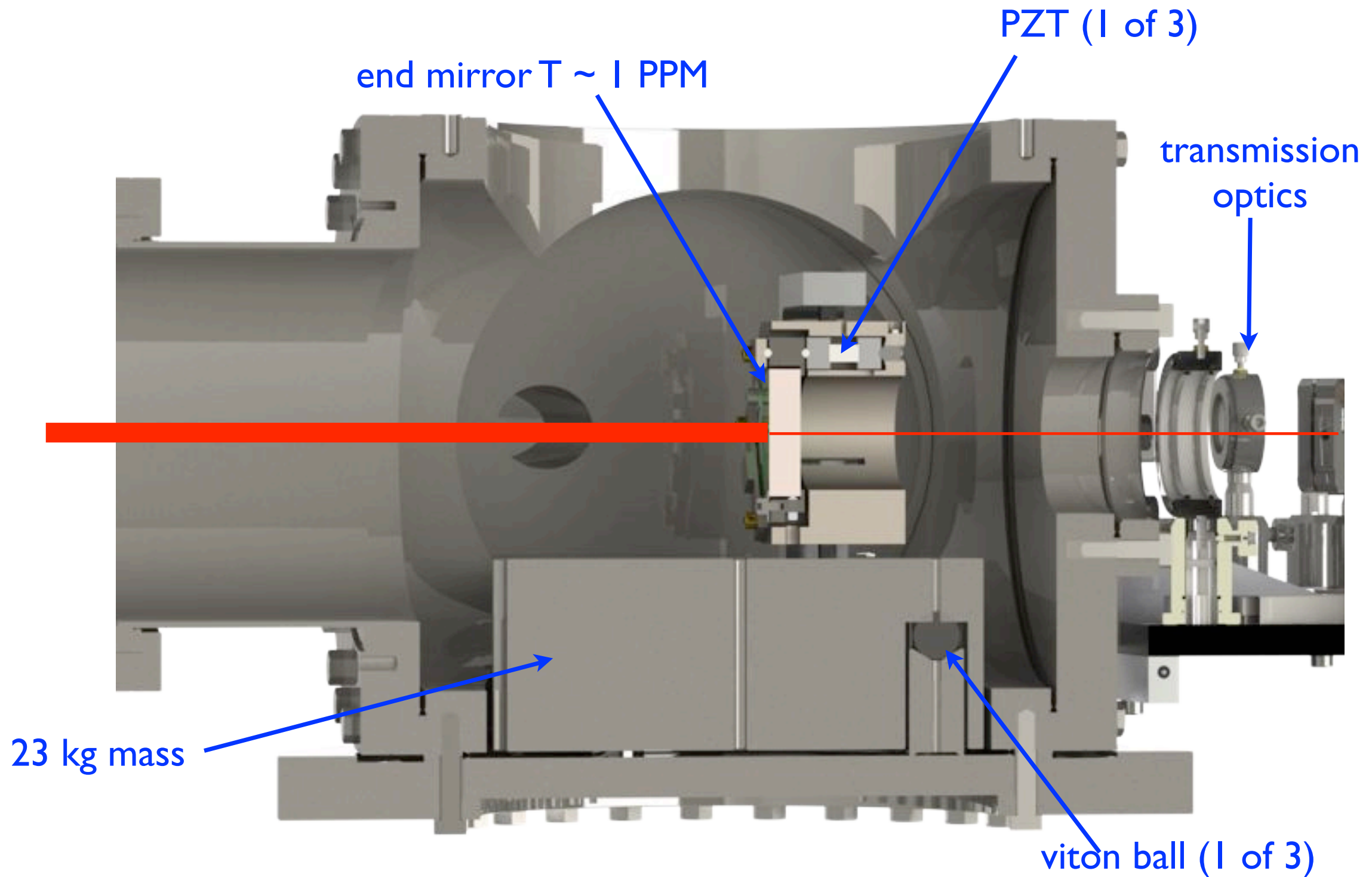
Seismic Isolation

Passive Seismic Isolation



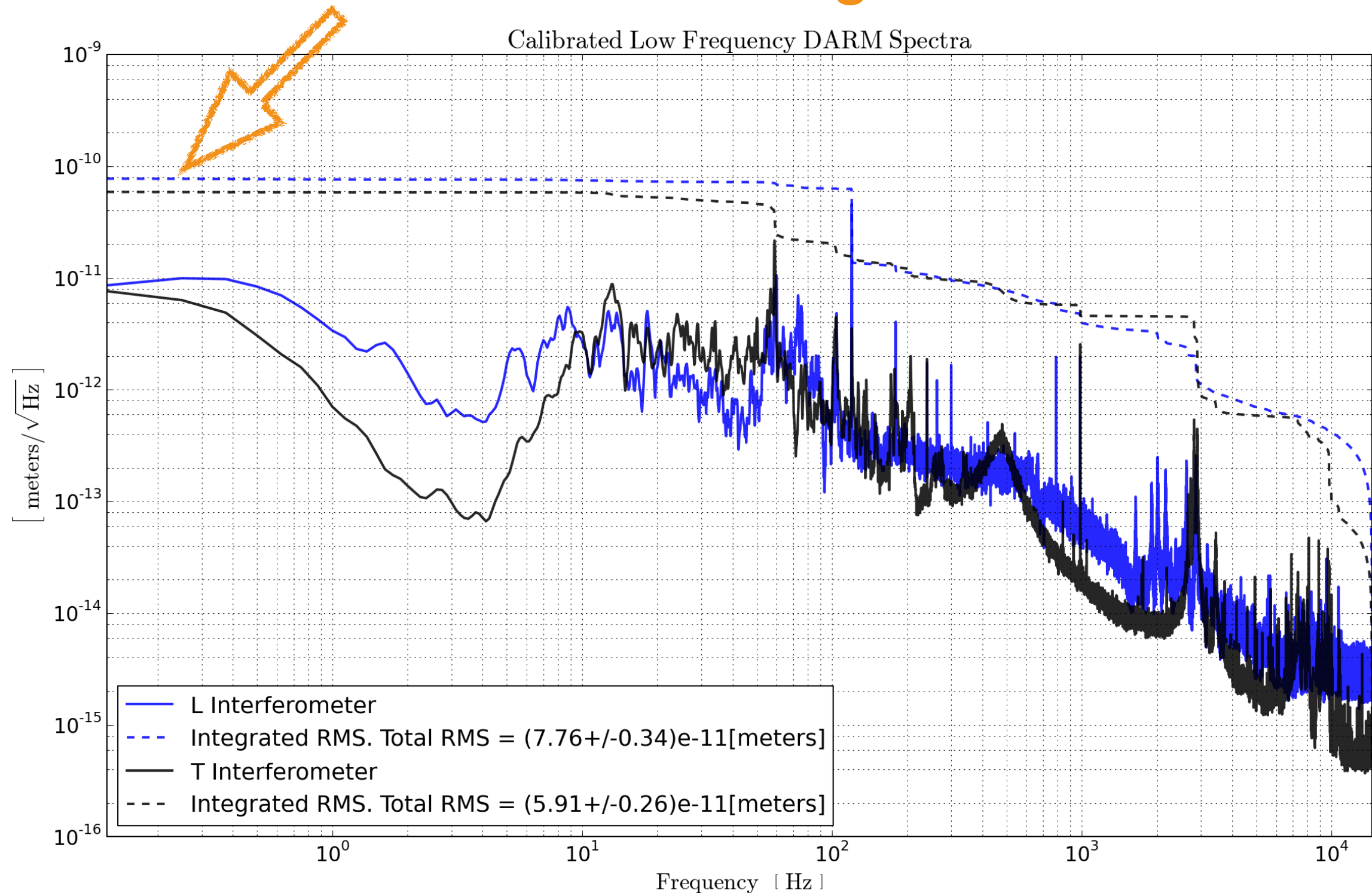
Seismic Isolation

End station optics and vibration isolation

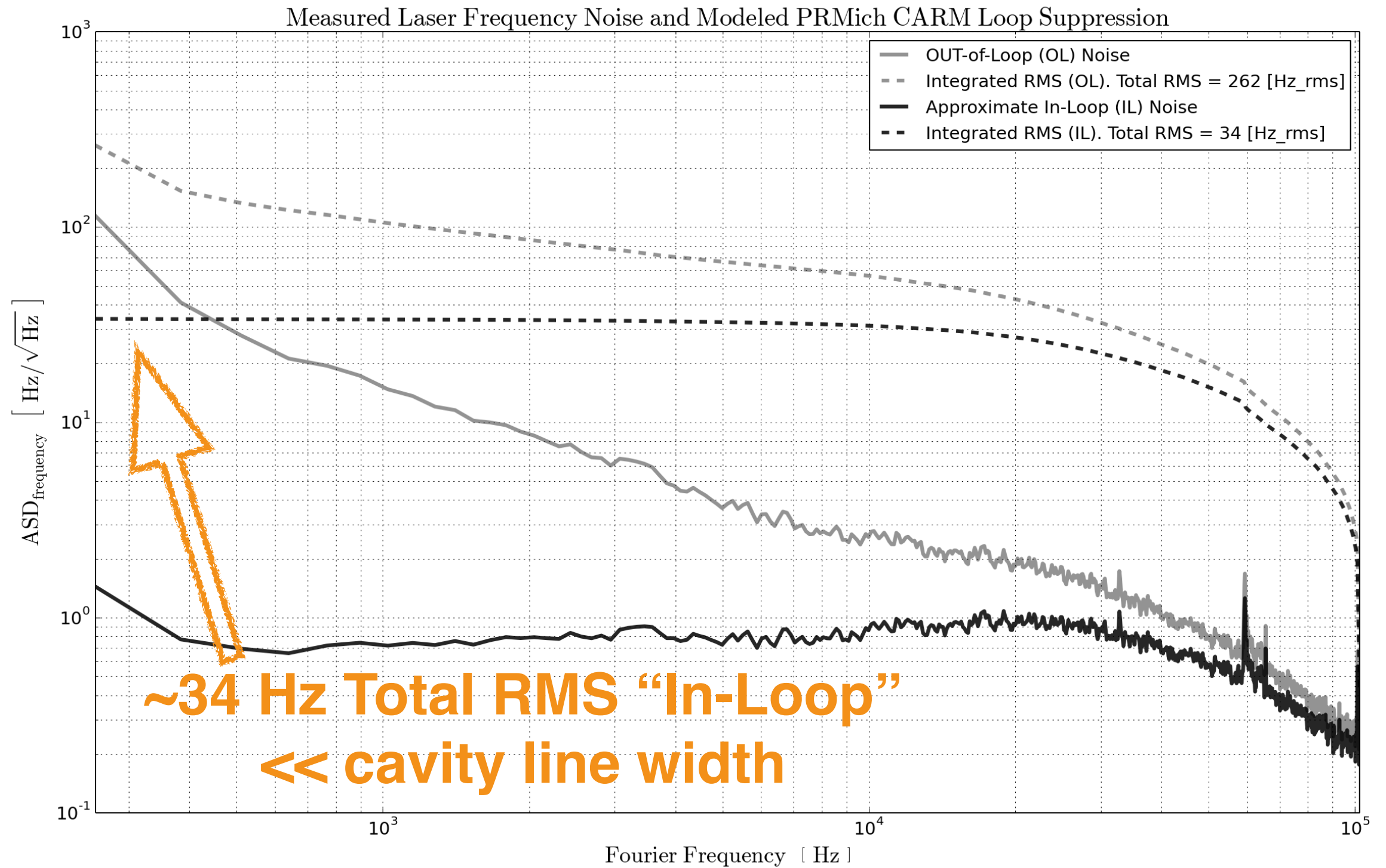


Low Frequency Residual DARM Motion

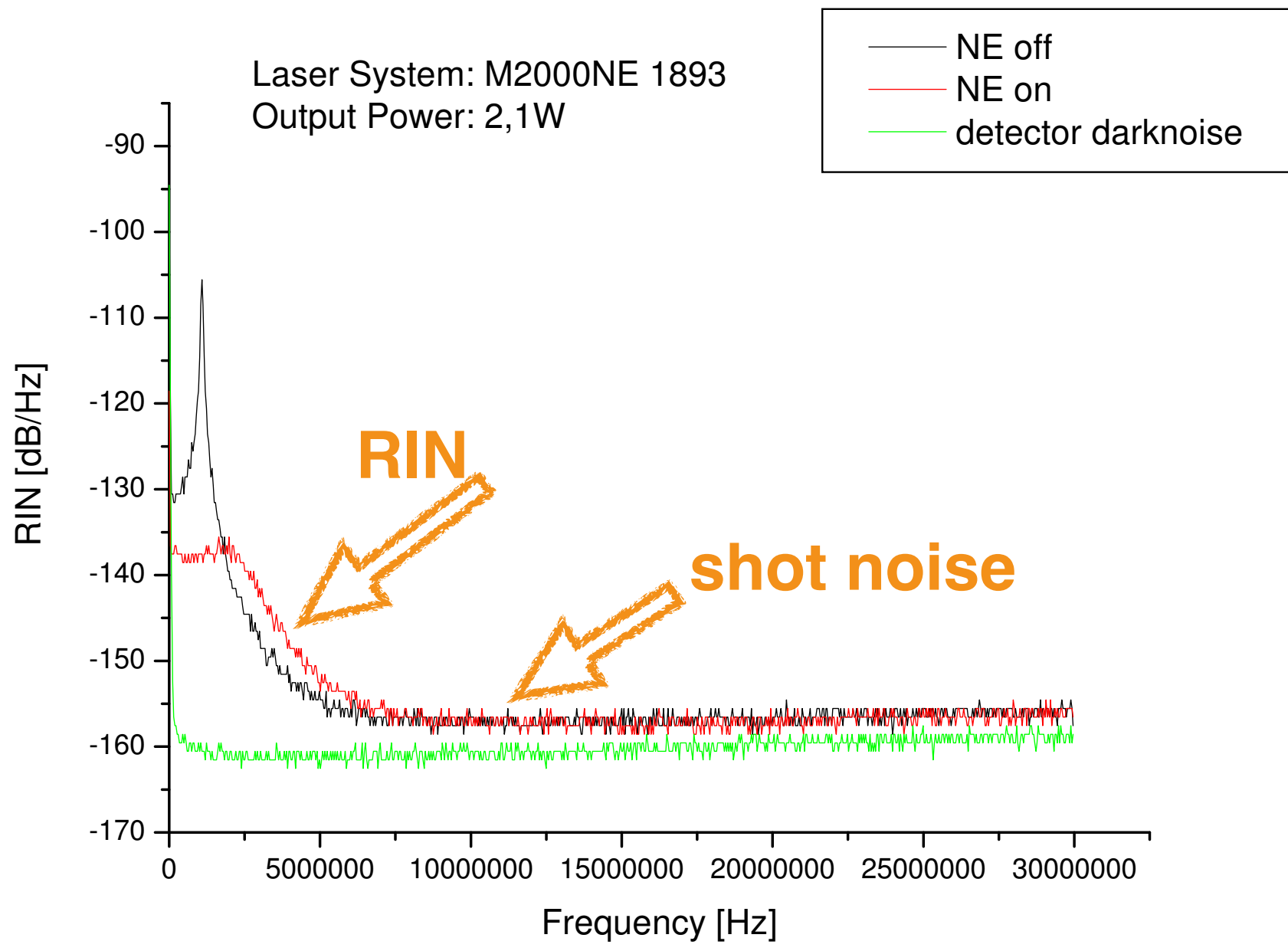
The TOTAL RMS motion is < 1 Angstrom!



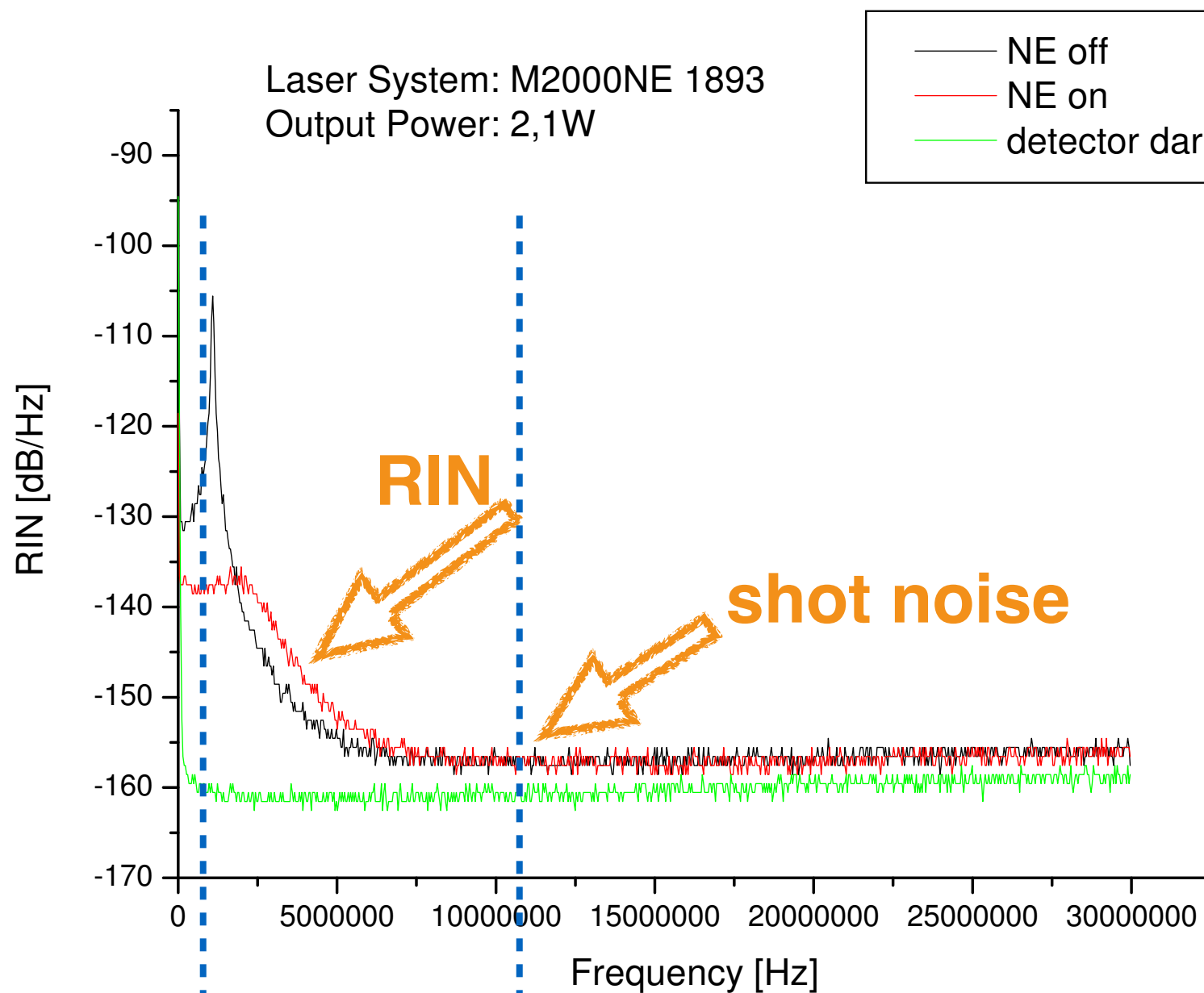
Laser Frequency Noise



Laser Relative Intensity Noise (RIN)



Laser Relative Intensity Noise (RIN)



> x2000 suppression of RIN by power-recycling cavity

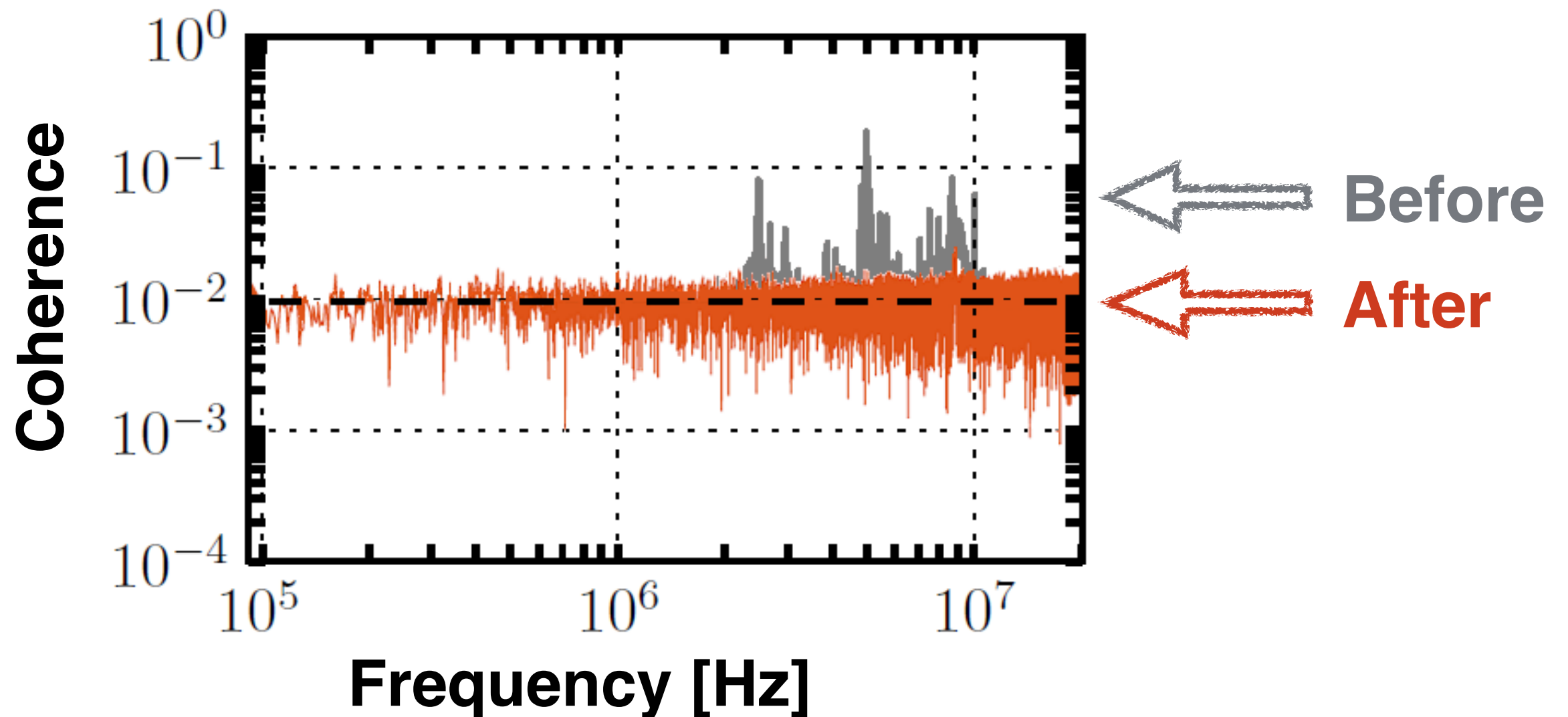
====> intensity noise below shot noise at interferometer output in our signal band

Signal Band

Radio Frequency Interference (RFI)

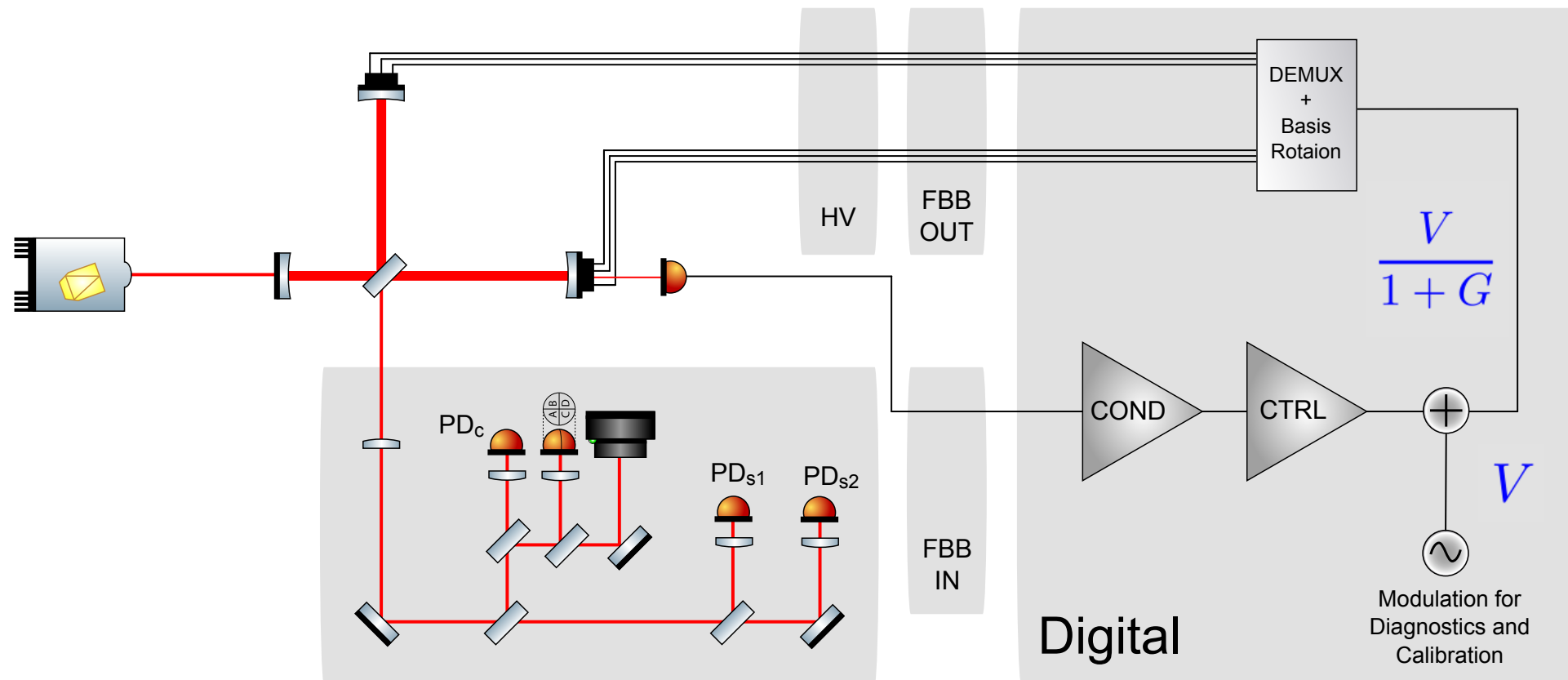
Extensive campaign to
reduce RFI correlations!

Correlations between the
2 lasers after 12 hrs of integration



End-To-End Calibration

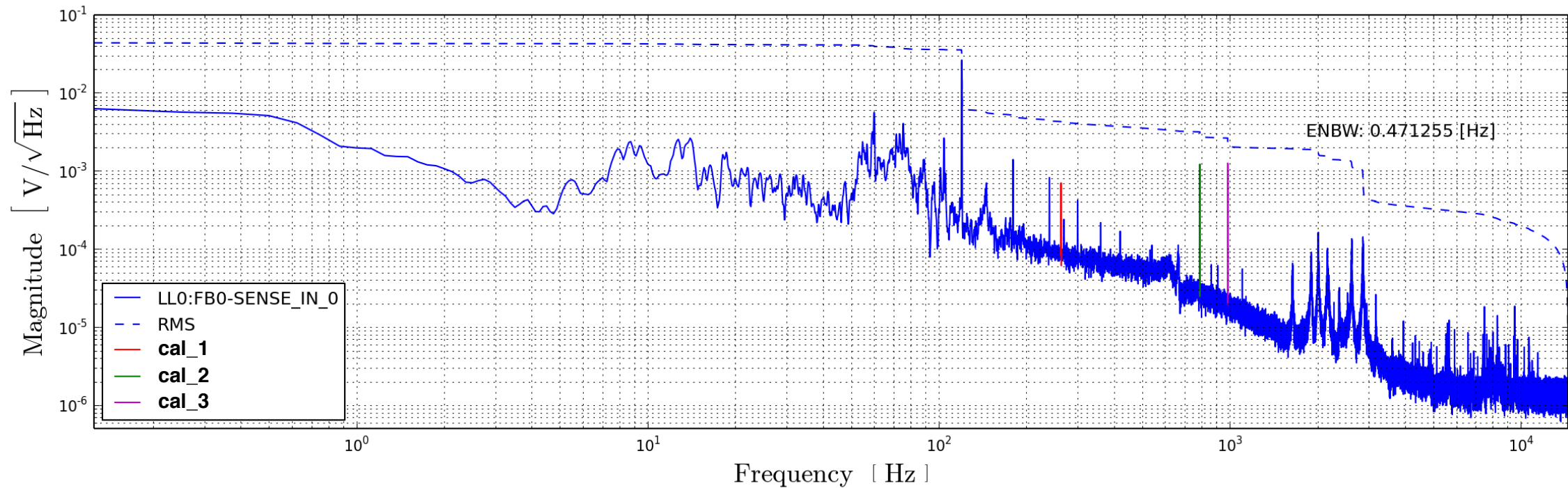
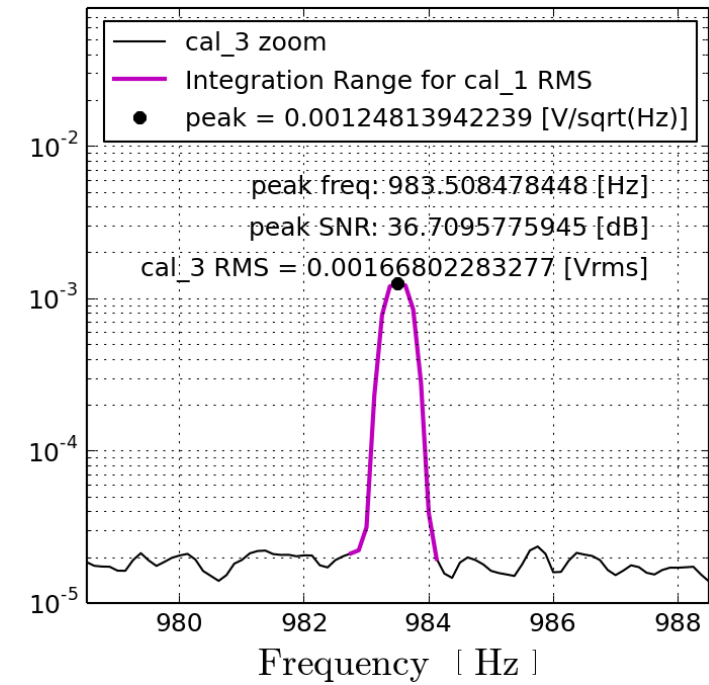
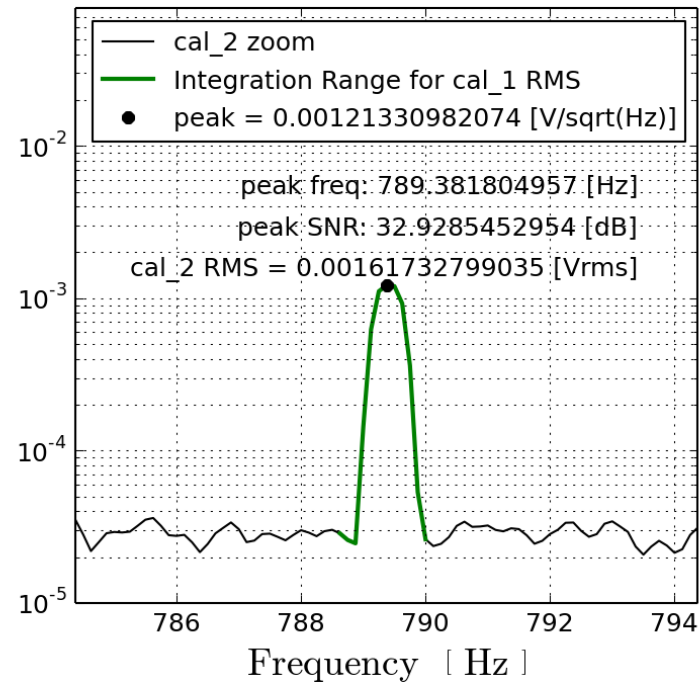
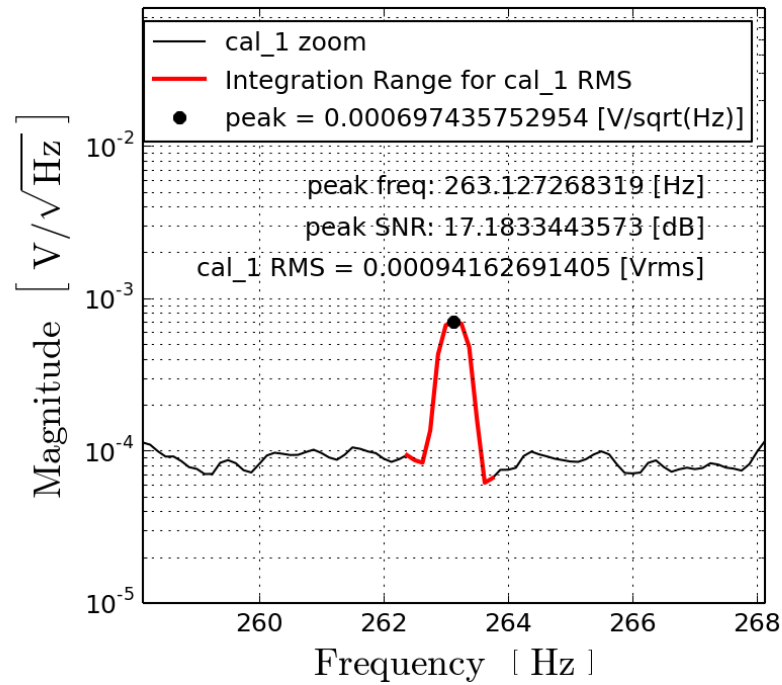
End-To-End Calibration



- Drive a low frequency DARM calibration line
- Measure the line precisely using Michelson (no power-recycling)
- Measure effects of control loop on calibration line
- Transfer low frequency line to high frequency on signal photodetectors

End-To-End Calibration

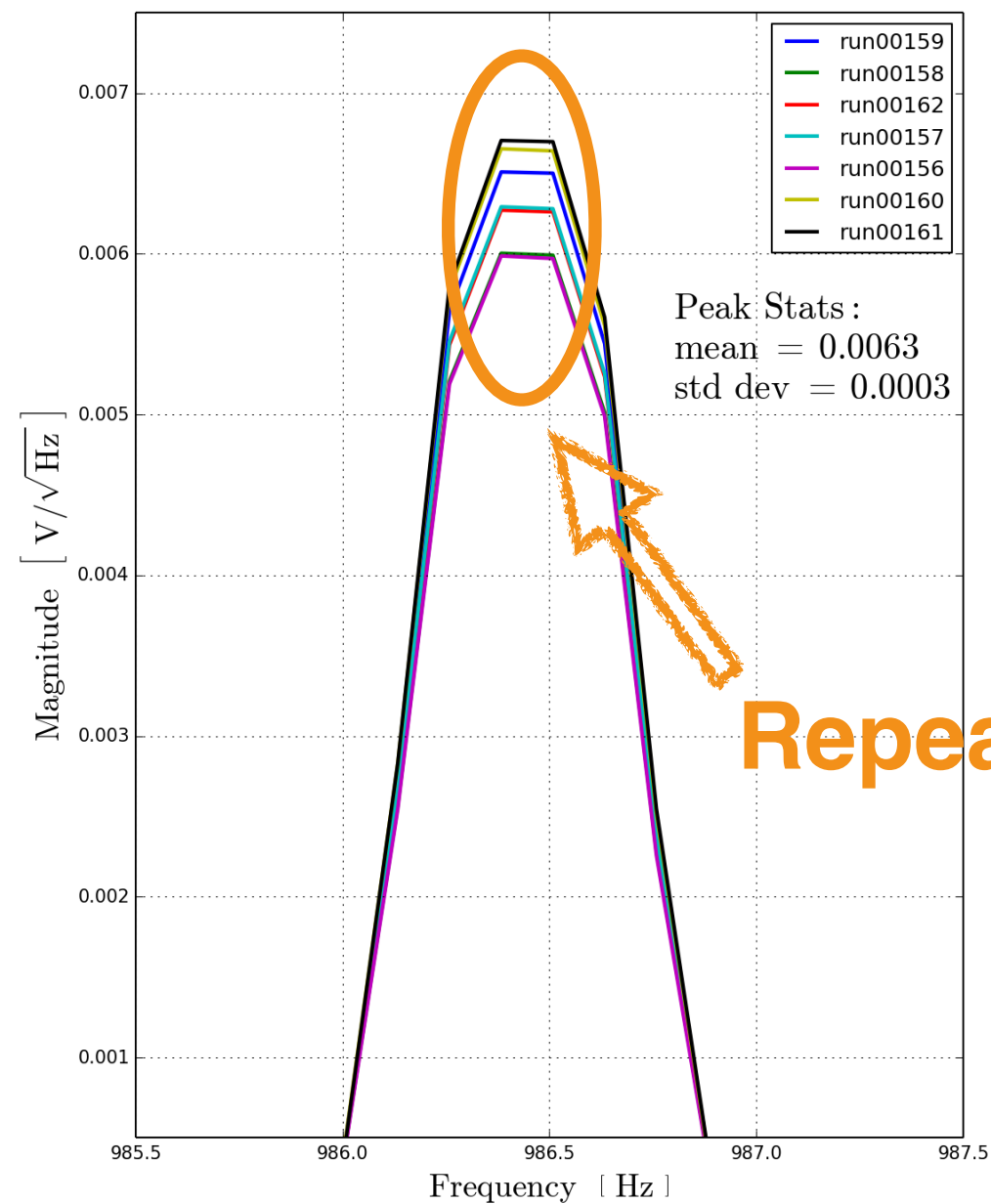
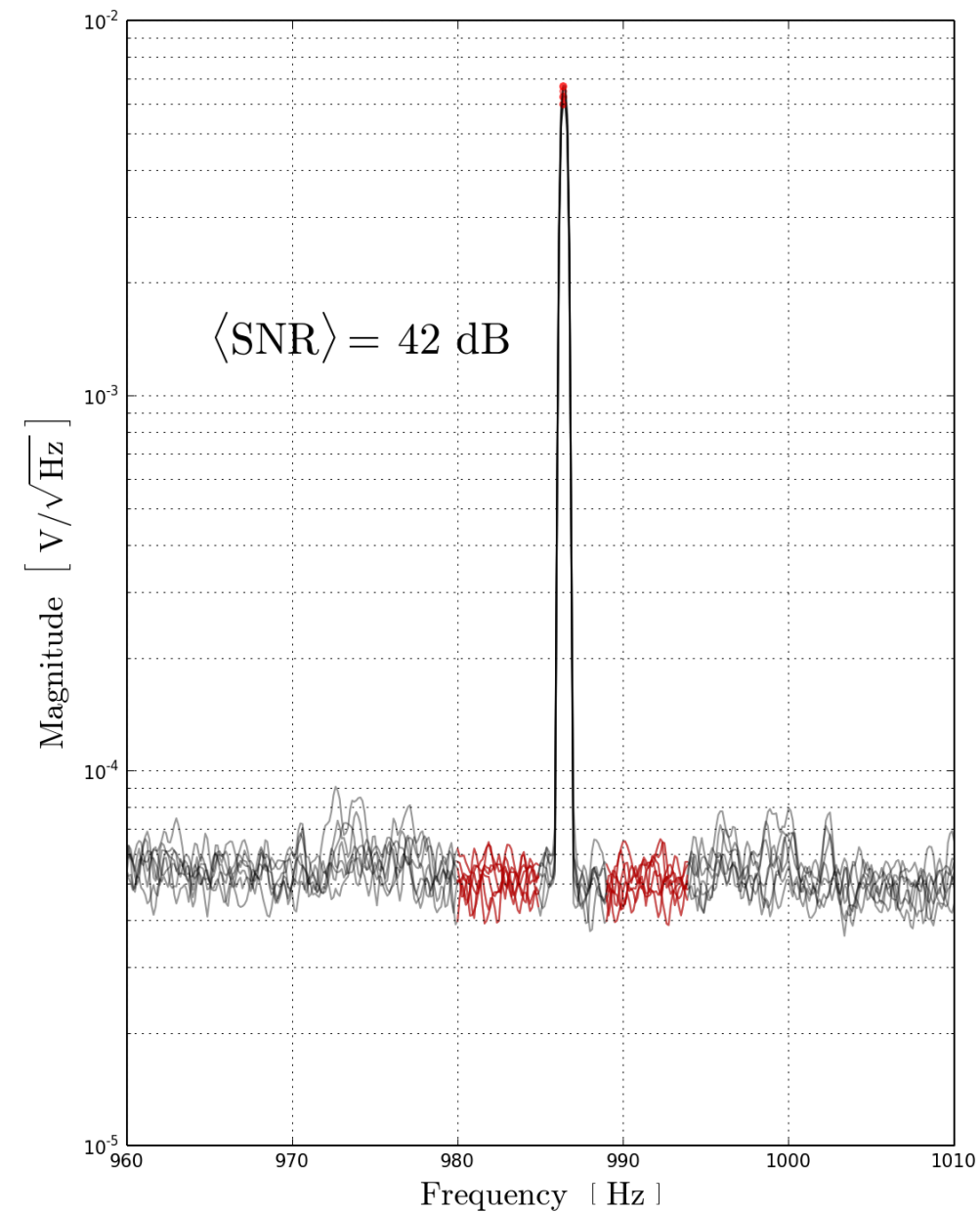
In-Loop Calibration Lines in PRMichelson DARM Spectrum



End-To-End Calibration

Total Error for the
2 interferometers:
7% and 8%

Power Recycled Calibration Line: DAQ Runs 00156–00162



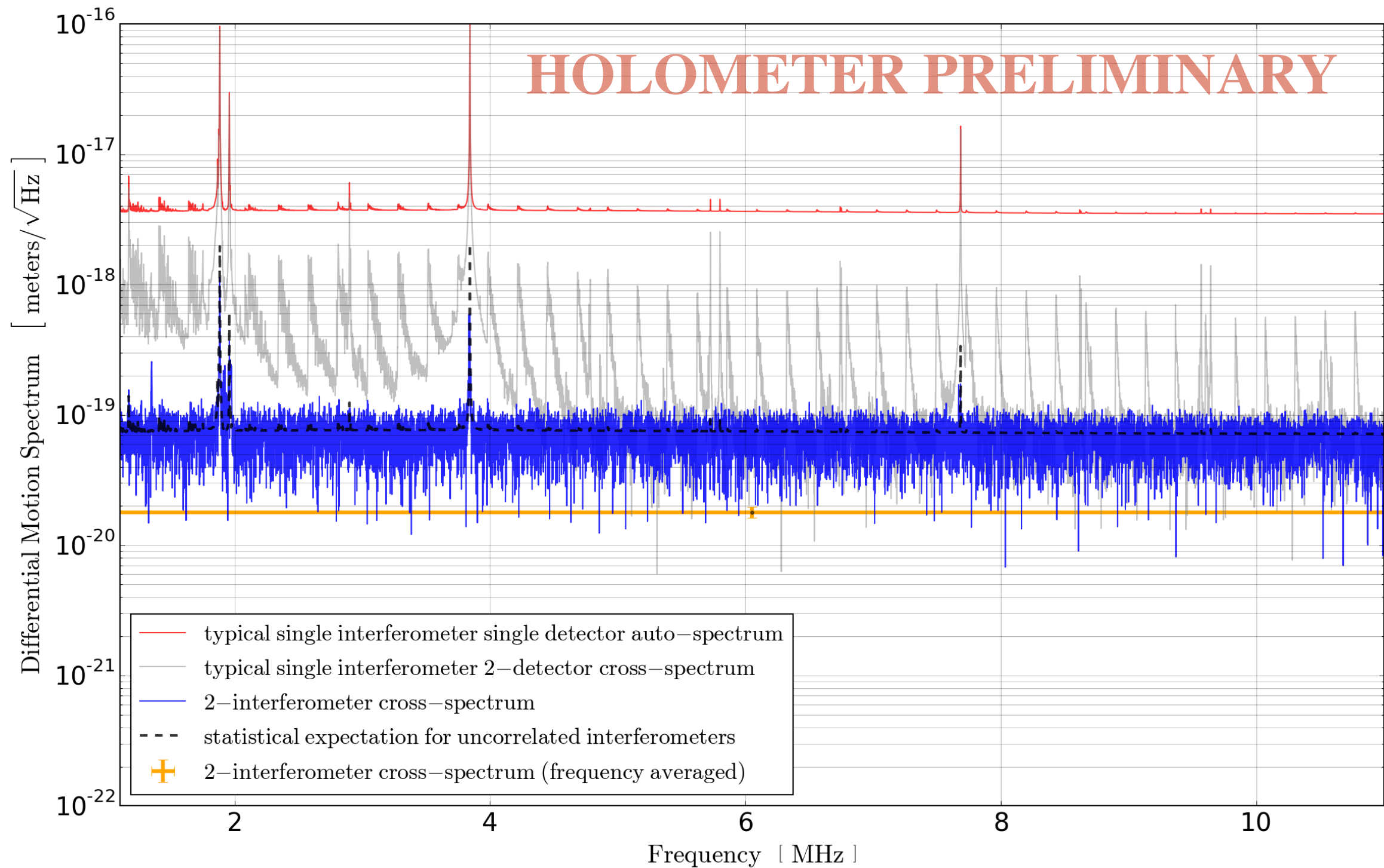
Repeatable to 4%

Analysis and Results

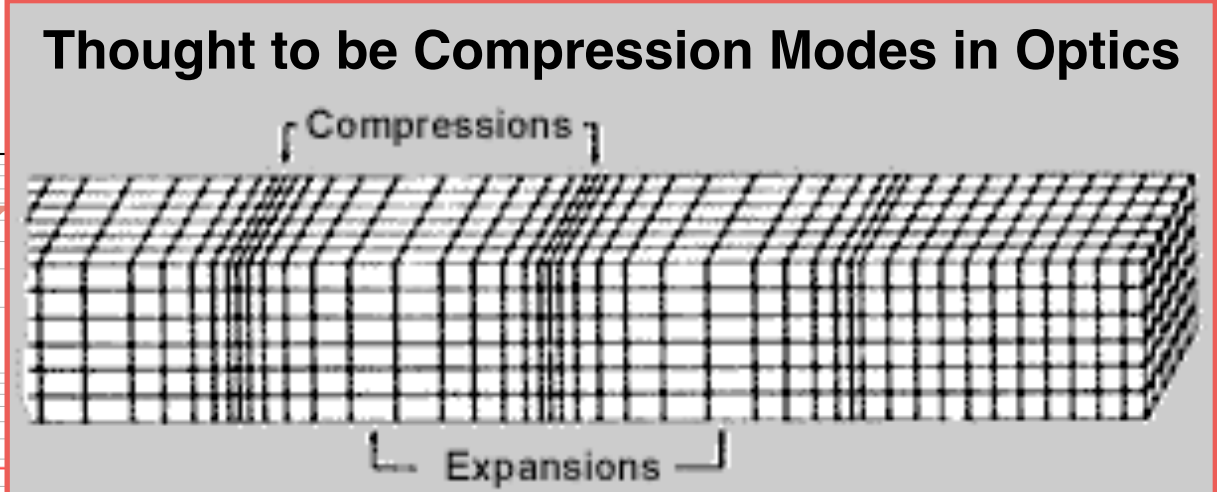
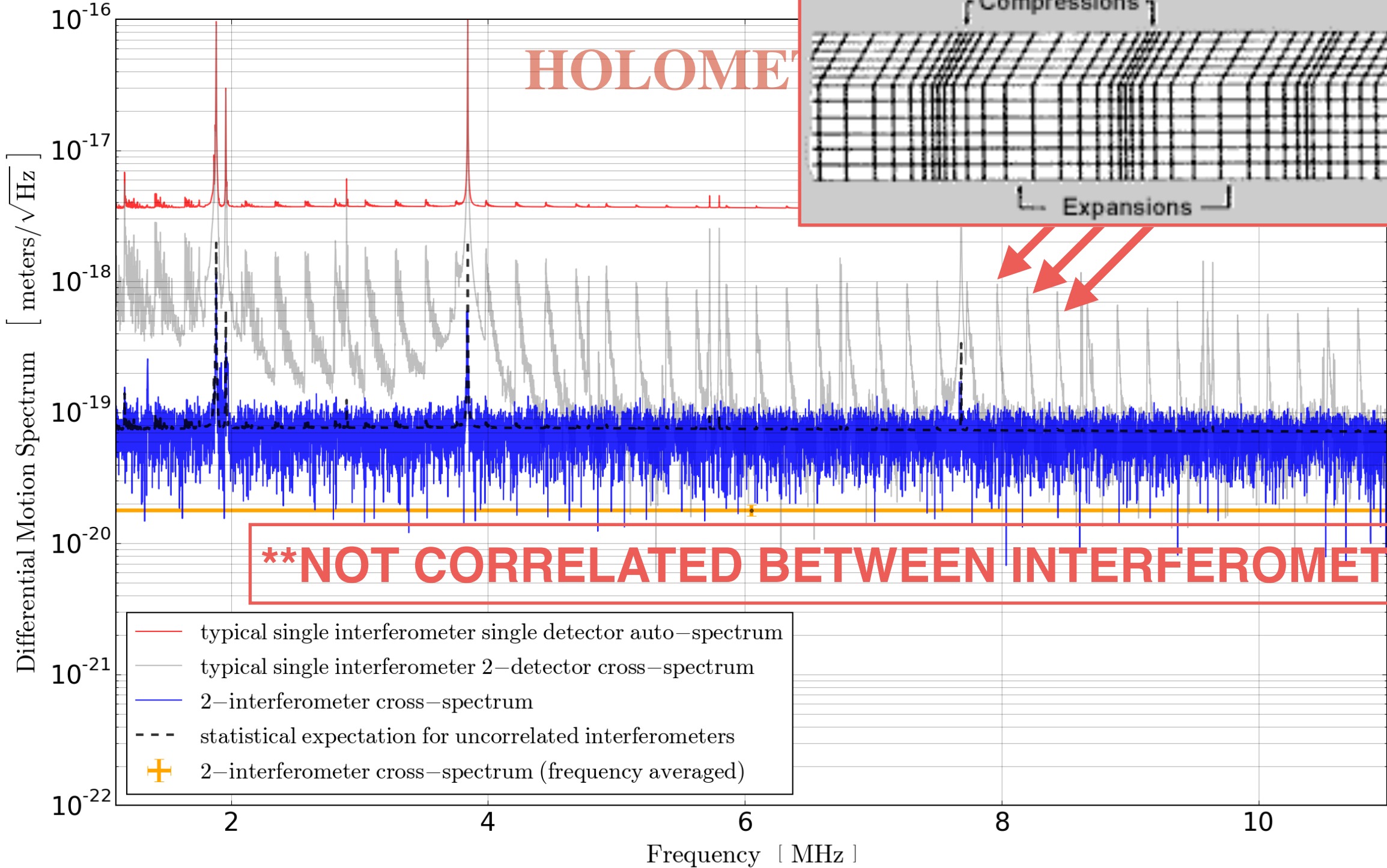
Data Acquisition and Methodology

- Digitize 4 signal photodetectors + 2 auxiliary channels at 100MHz
- Compute Fourier Transforms + Cross-Spectra between all channels for each 1 second long data segment, **in real time**
- 763Hz frequency resolution for this data set
- The resulting (real-valued) auto-spectra and (complex-valued) cross-spectra, in power spectral density units [V^2/Hz], are then averaged in the frequency domain for each successive 1 second long batch of data
- Apply Differential Arm sensitivity calibration in meters/Volt
- Perform Gravitational Wave Upper Limit statistical analysis

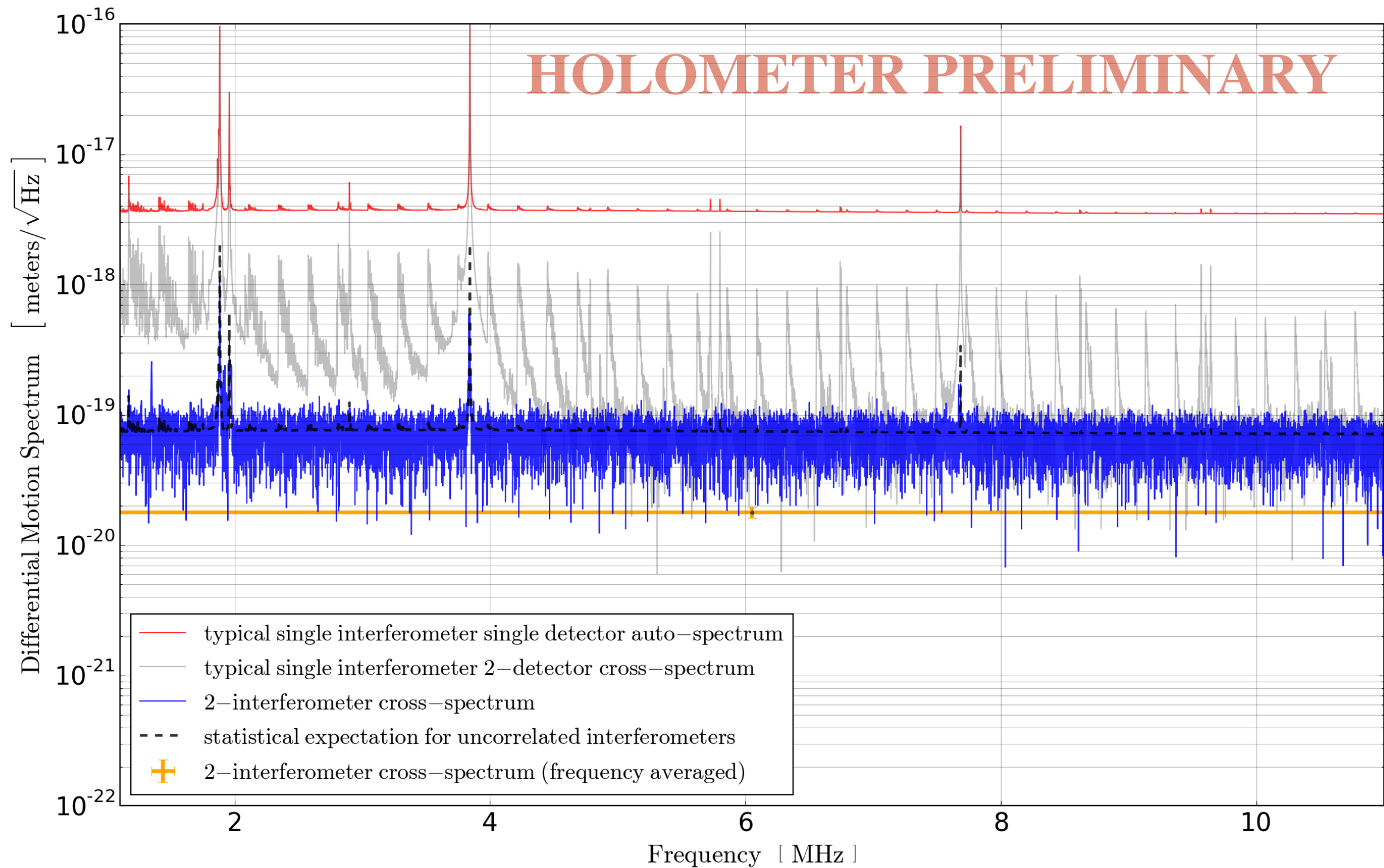
Differential Arm Motion Sensitivity



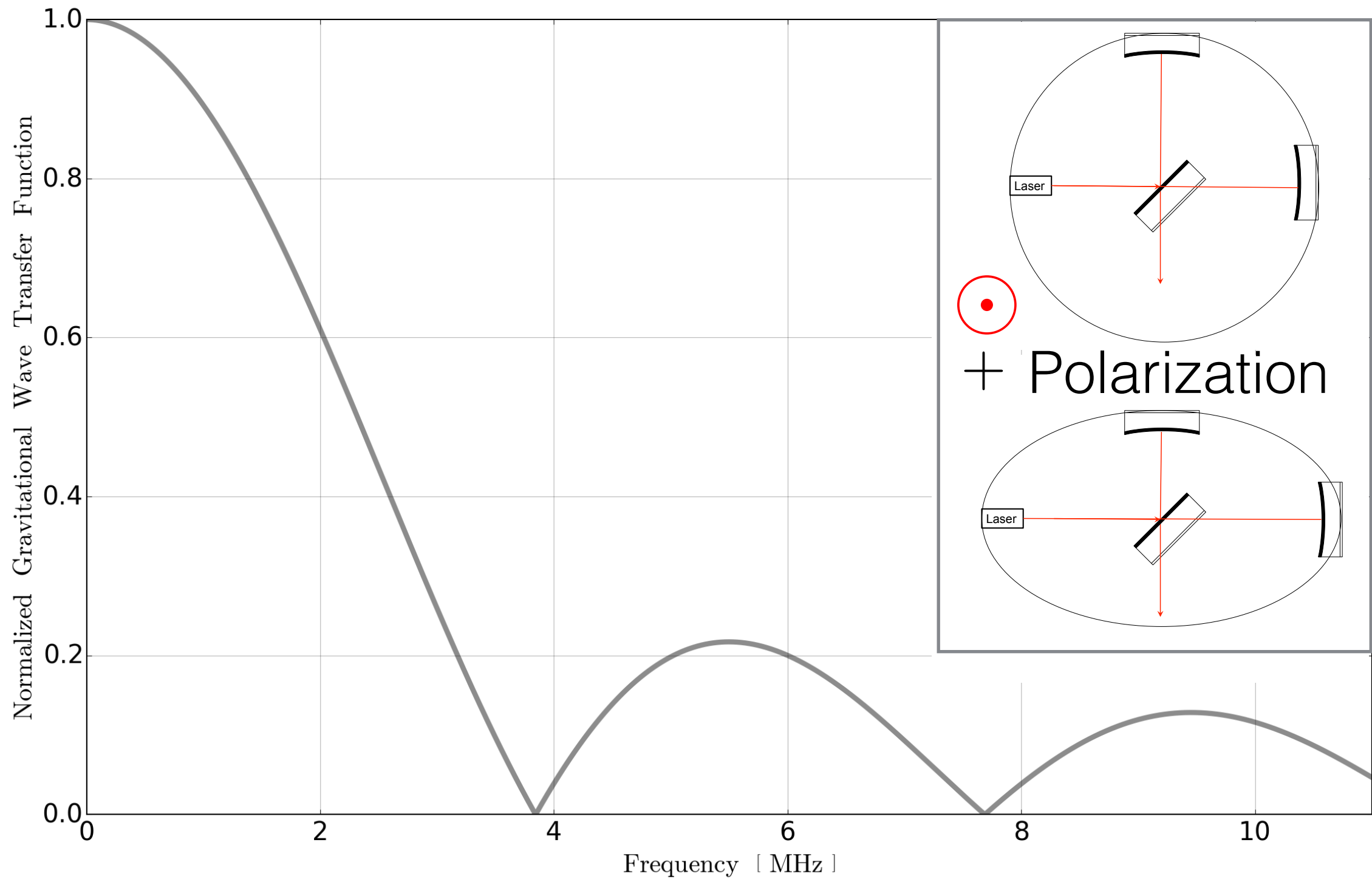
Differential Arm Motion Sensitivity

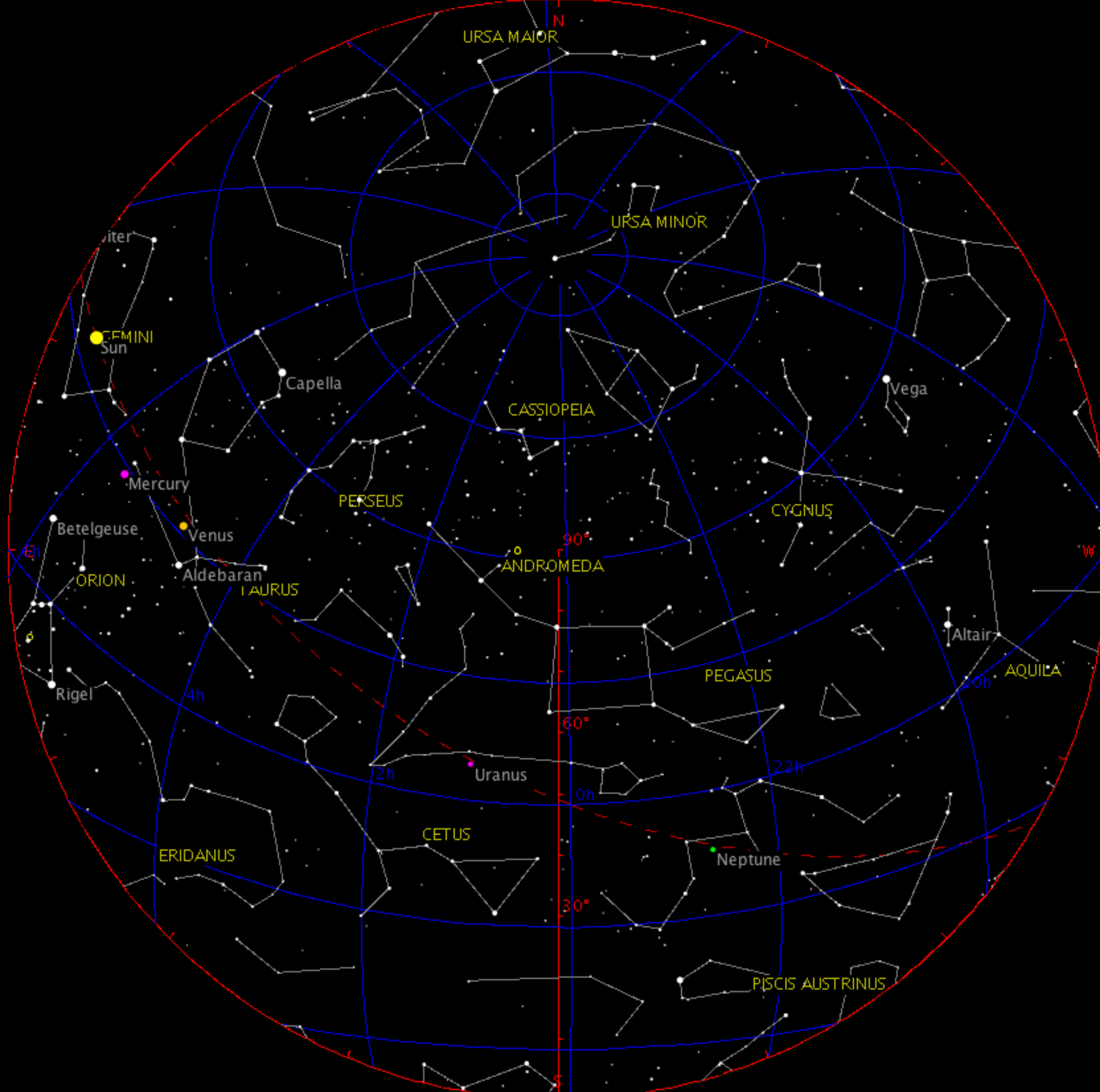


Differential Arm Motion Sensitivity

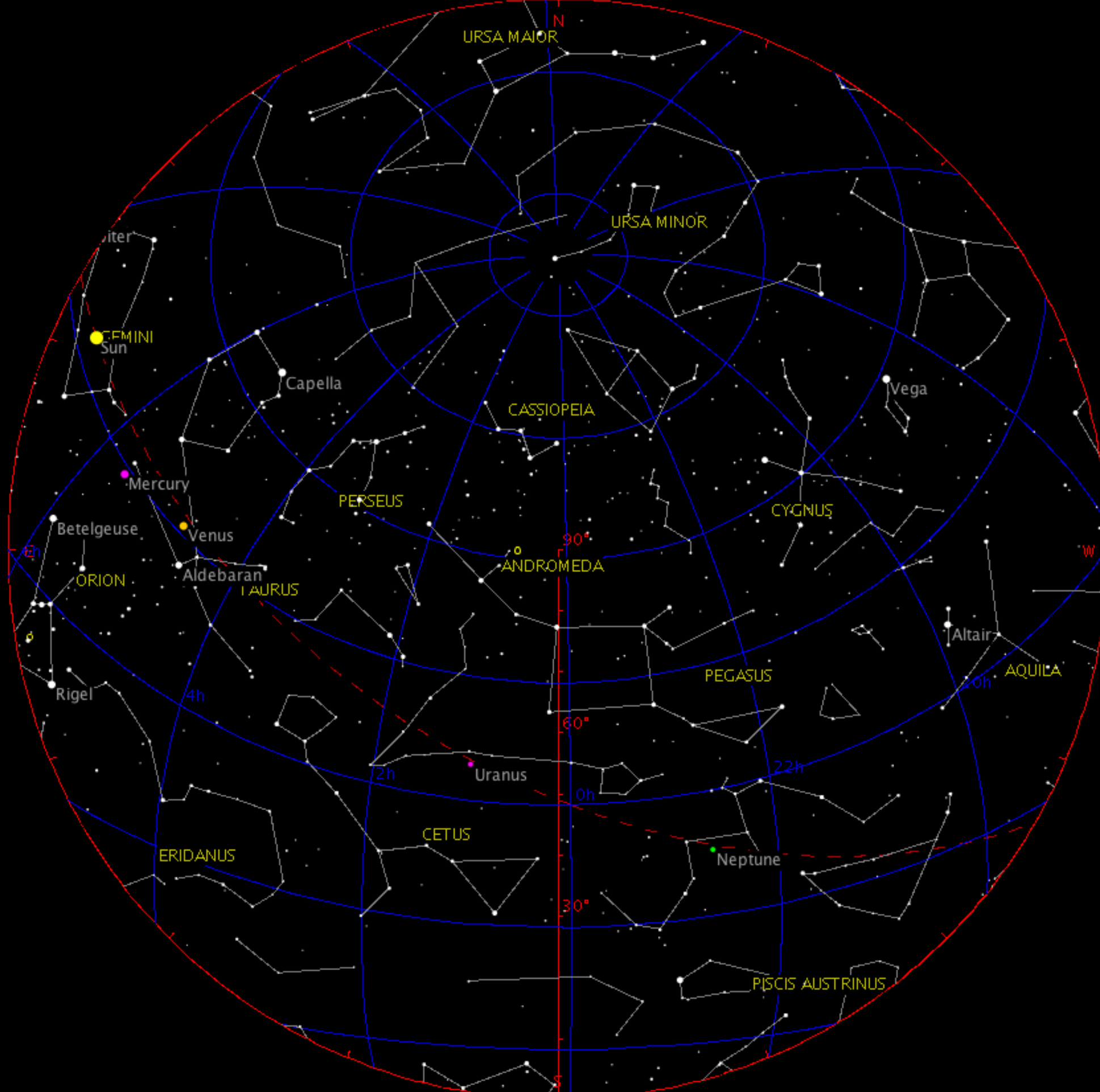


Detector Response to Gravitational Waves in the “Optimal Orientation”

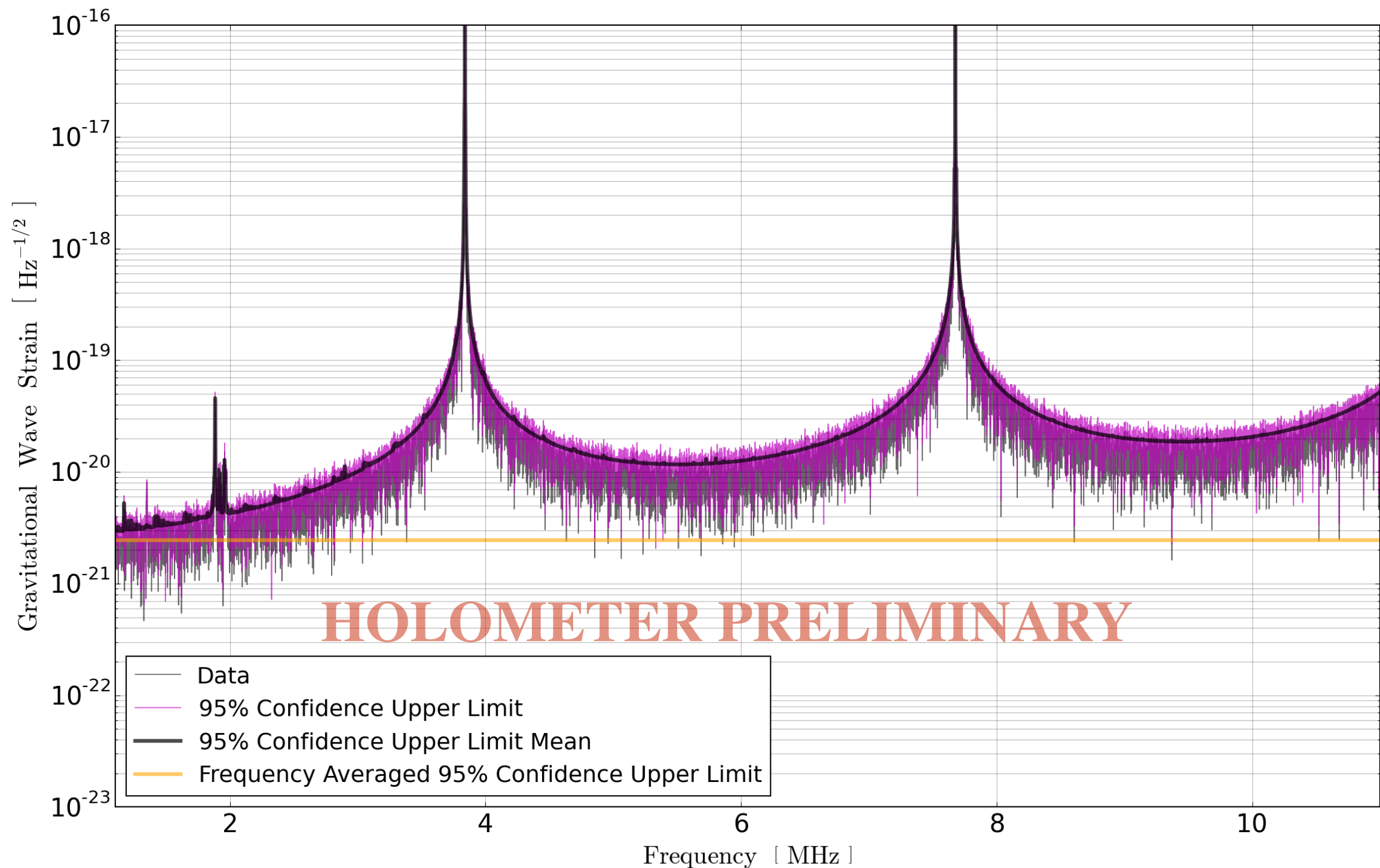




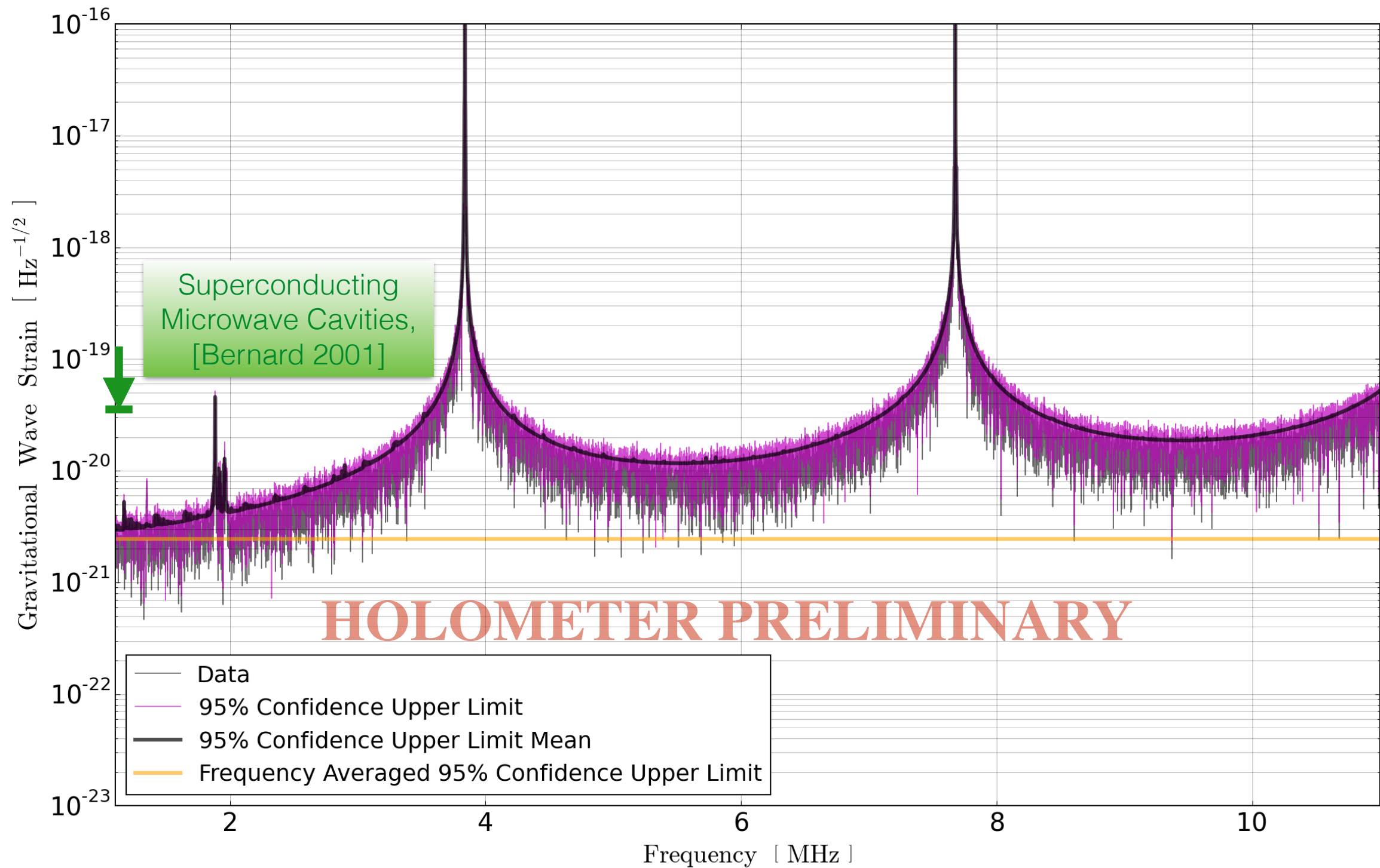
Animated



95% Confidence Upper Limits on Strain Amplitude of Gravitational Waves



Comparison With Previous High Frequency GW Limits



Where The New Results Fit In

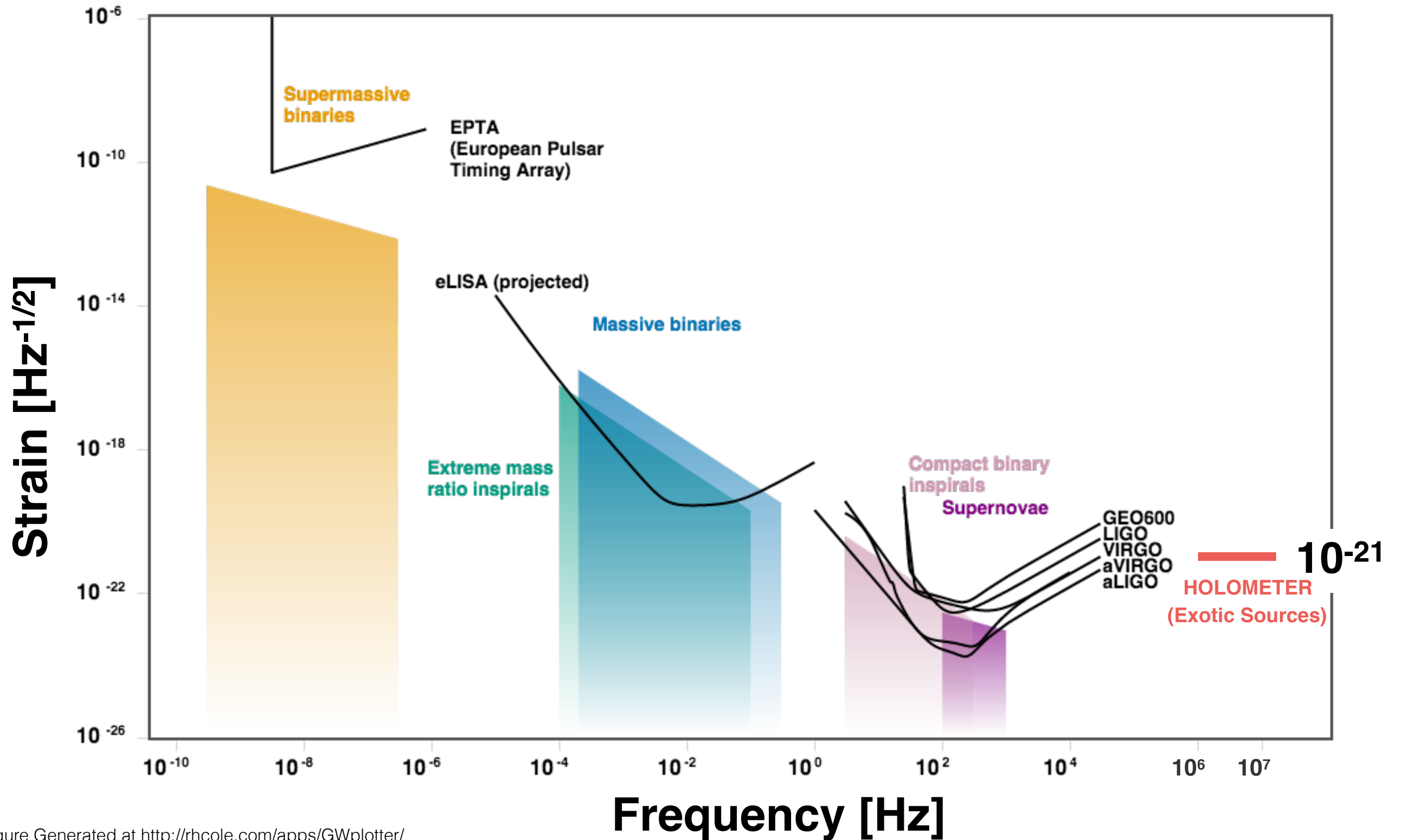


Figure Generated at <http://rhcole.com/apps/GWplotter/>
 See also: C J Moore et al 2015 Class. Quantum Grav. 32 015014
 doi:10.1088/0264-9381/32/1/015014

The Holometer Collaboration



The Holometer Team, pictured over the East Holometer arms. From left to right: C. Hogan, S. Meyer, R. Weiss, R. Lanza, D. Gustafson, H. Glass, J. Richardson, L. McCuller, A. Chou, B. Kamai, C. Stoughton, O. Kwon, R. Tomlin

Thank You!